Vaccine 28S (2010) B60–B67

Contents lists available at ScienceDirect

Vaccine

journal homepage: www.elsevier.com/locate/vaccine

HIV-2 capsids distinguish high and low virus load patients in a West African community cohort

Clayton O. Onyango[a], Aleksandra Leligdowicz[a,b], Masaru Yokoyama[c], Hironori Sato[c], Haihan Song[d], Emi E. Nakayama[d], Tatsuo Shioda[d,*], Thushan de Silva[a], John Townend[a], Assan Jaye[a], Hilton Whittle[a], Sarah Rowland-Jones[a,b], Matthew Cotten[a,*]

[a] Medical Research Council Laboratories, Fajara, Atlantic Road, P.O. Box 273, The Gambia
[b] Weatherall Institute of Molecular Medicine, Medical Research Council Human Immunology Unit, John Radcliffe Hospital, Oxford, OX3 9DS, United Kingdom
[c] Laboratory of Viral Genomics, Center for Pathogen Genomics, National Institute of Infectious Diseases, Tokyo 208-0011, Japan
[d] Department of Viral Infections, Research Institute for Microbial Diseases, Osaka University, Osaka 565-0871, Japan

ARTICLE INFO

Article history:
Received 15 May 2009
Received in revised form 13 August 2009
Accepted 17 August 2009

Keywords:
HIV-2
Capsid
TRIM5α

ABSTRACT

HIV-2 causes AIDS similar to HIV-1, however a considerable proportion of HIV-2 infected patients show no disease and have low plasma virus load (VL). An analysis of HIV-2 capsid (p26) variation demonstrated that proline at p26 positions 119, 159 and 178 are more frequent in lower VL subjects while non-proline residues at all three sites are more frequent in subjects with high VL. *In vitro* replication levels of viruses bearing changes at the three sites suggested that these three residues influence virus replication by altering susceptibility to TRIM5α. These results provide new insights into HIV-2 pathogenesis.

1. Introduction

HIV-2 was discovered in West Africa patients [1,2] shortly after the discovery of HIV-1, with HIV-2 entering humans via zoonoses distinct from the entry of HIV-1 some time in the early 20th century [3]. The two viruses have 60–80% sequence homology and have similar genomic organization, yet the viruses have distinct transmission rates and disease associations (reviewed in Ref. [4]). Although some HIV-2-infected patients progress to AIDS, the majority control infection [5–7] and patients with low VL survive longer [8]. Early descriptions of HIV-2 observed differences in the virus genetics [9] and noted that the HIV-2 epidemic behaved liked a mixture of pathological and non-pathological viruses [5,10]. Studying and understanding HIV-2 represents a possibility to discover how a potentially lethal lentivirus infection can be controlled by humans.

There are limited data on HIV-2 sequence variation associated with either long-term control or progression to disease [9,11,12]. Although some correlation of Nef variation with disease has been observed [13], most HIV-2 sequences in the public databases are derived from viruses isolated from AIDS patients where high VLs facilitate virus isolation and sequencing which could introduce bias in the data. Sequences derived from patients with low VL are essential for understanding disease non-progression in HIV-2 infection. A community cohort to study HIV was established in Caio, Guinea Bissau in 1988 [50], reviewed in Ref. [4]. HIV screening of the entire adult population in the Caio community cohort have identified HIV-2-positive subjects with a wide spectrum of clinical symptoms and survival [4,10,14]; a sequence analysis of the virus among these patients could identify virus variations that influence outcome.

The capsid (CA) protein (p24 in HIV-1; p26 in HIV-2) has a structure that is conserved among retroviruses [15,16]. p26 accumulates during replication as a Gag polyprotein, assembles into spherical structures that package viral RNA and is subsequently processed by the viral protease and reassembled into the mature virus cores [16–18]. The CA has a distinct amino-terminal domain (residues 1–145), that is exposed on the surface of cores, and a C-terminal domain (residues 146–230) which is required for oligomerization [19]. The 20 amino acid major homology region (MHR) in the C-terminal domain is highly conserved; changes in this motif can interfere with CA assembly, maturation and early stages of infec-

* Corresponding authors.
E-mail addresses: conyango@mrc.gm (C.O. Onyango), aleksandra.leligdowicz@mail.mcgill.ca (A. Leligdowicz), yokoyama@nih.go.jp (M. Yokoyama), hirosato@nih.go.jp (H. Sato), haihansong@hotmail.com (H. Song), emien@biken.osaka-u.ac.jp (E.E. Nakayama), shioda@biken.osaka-u.ac.jp (T. Shioda), tdesilva@mrc.gm (T. de Silva), jtownend@mrc.gm (J. Townend), ajaye@mrc.gm (A. Jaye), hwhittle@mrc.gm (H. Whittle), sarah.rowland-jones@ndm.ox.ac.uk (S. Rowland-Jones), mcotten@mrc.gm (M. Cotten).

0264-410X/$ – see front matter © 2009 Elsevier Ltd. All rights reserved.
doi:10.1016/j.vaccine.2009.08.060

Table 1
Comparison of the cohort p26 residues 119, 159 and 178 to HIV-2_{ROD} p26; variation with viral load.

ID	Source	VL	119	159	178	ID	Source	VL	119	159	178
ROD			P	P	P	ROD			P	P	P
CO310	RNA	<100	.	.	.	CO309	RNA	283	Q	S	.
CO315	DNA	<100	.	.	.	CO316	RNA	372	.	.	.
CO318	PRO	<100	.	.	.	CO364	RNA	387	A	.	.
CO319	RNA	<100	.	.	.	CO314	DNA	393	.	S	.
CO324	RNA	<100	.	.	.	CO354	DNA	413	.	.	.
CO326	RNA	<100	.	.	.	CO323	RNA	497	A	.	.
CO327	DNA	<100	.	.	.	CO365	RNA	523	A	S	A
CO339	RNA	<100	.	.	.	CO350	RNA	540	A	S	A
CO349	RNA	<100	.	.	.	CO322	RNA	610	.	S	A
CO359	RNA	<100	.	.	.	CO355	RNA	651	A	.	A
CO360	RNA	<100	.	.	.	CO357	RNA	813	A	S	Q
CO344	DNA	<100	A	.	.	CO332	RNA	1085	A	.	V
CO346	DNA	<100	A	.	.	CO305	RNA	1343	A	.	.
CO351	RNA	<100	A	.	.	CO340	RNA	1587	.	.	.
CO308	RNA	<100	Q	.	.	CO321	RNA	1608	.	.	.
CO337	DNA	<100	.	T	.	CO342	RNA	1907	A	S	.
CO361	RNA	<100	A	S	.	CO325	RNA	1999	.	.	.
CO366	RNA	<100	A	S	.	CO330	RNA	2653	A	S	.
CO367	DNA	<100	A	S	.	CO331	RNA	2949	A	S	A
CO363	DNA	<100	Q	S	.	CO320	RNA	3241	A	.	.
CO335	RNA	<100	A	.	A	CO307	RNA	3764	G	S	.
CO336	RNA	<100	A	.	A	CO368	RNA	6431	A	T	S
CO341	RNA	<100	A	.	A	CO345	RNA	9659	A	.	.
CO362	DNA	<100	A	.	A	CO312	RNA	9979	A	S	A
CO301	DNA	<100	A	S	.	CO334	RNA	10752	.	S	.
CO306	DNA	<100	A	S	A	CO311	RNA	14104	A	S	A
CO333	RNA	<100	A	S	A	CO313	RNA	17067	A	S	A
CO302	RNA	109	.	.	.	CO369	RNA	22446	Q	S	.
CO304	DNA	114	.	.	.	CO343	RNA	25836	A	S	.
CO303	RNA	154	A	S	A	CO338	RNA	28581	Q	S	A
CO356	DNA	182	.	.	.	CO317	RNA	37503	A	S	A
CO328	RNA	198	A	.	.	CO347	RNA	146284	A	.	.
CO353	DNA	234	.	.	.	CO348	RNA	148593	A	.	A
CO329	RNA	267	A	S	S	CO358	RNA	283542	A	S	.
CO352	RNA	275	.	S	.						

Samples from 69 HIV-2 singly-infected patients collected in 2006 were used for sequencing (see Section 2). Patient plasma VL was assayed by RT-PCR with a lower limit of detection of 100 virus copies/ml. For statistical analysis, undetectable viremia was given a value of 50 copies/ml. Viral loads (copies/ml) are indicated in second column. The source of template for the PCR reaction (circulation RNA (RNA) or proviral DNA (DNA)) is indicated. The reference sequence derived from HIV-2_{ROD} p26 is listed in the first row, in the subsequent rows identity with the HIV-2_{ROD} p26 sequence is indicated with a period (.).

tion [19,20]. The multiple functions impose strict constraints on the amino acid changes allowed in CA. Studying the limited variations that do occur in p26 can provide important information on both protein function and the selective forces acting on HIV-2. In this study, we have tested the hypothesis that HIV-2 p26 capsid variants modulate HIV-2 viral load.

2. Methods

2.1. Patient cohort.

Study subjects were recruited from the community-based cohort in Caio, Guinea Bissau (study subjects described in Ref. [14]). Briefly, HIV screening was performed with a Murex ICE HIV-1.2.0 immunoassay (Murex Diagnostics), confirmed and differentially diagnosed (HIV-1/HIV-2) using HEXAGON HIV (Human GmbH). Dually HIV-1+2 positive samples were subjected to peptide-based assays (Pepti-Lav 1-2, Sanofi Diagnostics Pasteur) and HIV-1 and HIV-2-specific polymerase chain reaction (PCR) with primers targeted to the long terminal repeats [7,8]. HIV-1+2 infected patients were excluded from the study. HIV-2 plasma viral load was quantified by PCR based method [7,21] with a lower limit of detection of 100 copies/ml, for analytic purposes, undetectable samples were assigned a value of 50 copies/ml. All participants were antiretroviral naïve at the time of the study and provided informed consent. The study was approved by the Gambian Government/MRC Ethics Committee, The Republic of Guinea Bissau Ministry of Health, and the Oxford Tropical Research Ethics Committee (OXTREC), UK.

2.2. p26 gene amplification strategy, optimization of primers.

p26 gene amplification primers were designed by selecting conserved sequences flanking the p26 coding region from all HIV-2 isolates in the Los Alamos HIV Database to be used as targets for PCR primers. Coupled reverse transcriptase and nested PCR reactions were performed with plasma-isolated virus RNA as template. The following primer sequences in various combinations were used for amplification:

MO017(OF, outer forward) GTCTGCGTCATTTGGTGCAT
MO018(IF, inner forward) CTGCAGAGAAAATGCCAAGCA
MO019(OR outer reverse) GGGCAGTTTGTCATGATGTGTCC
MO020(IR, inner reverse) GCCCTTCCTTTCCACAGTTCCA
MO021(IR) GCCCTTCCTTTCCACAATTCCA
MO030(OF)CACGCAGAAGAGAAAGTGAAAG
MO031(OR) CGGGGAAGTTGCGRGGCTT
MO032(IF) AGTAGACCAACAGCACCACC
MO036(OF) GTGGGCAGCGAATGAATTGG
MO037(OF) GTGGGCAGCGAACGAATTGG
MO038(OR) AAAGAGAGAATTGAGGTGCAGCA.

In case none of the primer combinations amplified a product from RNA, amplification of provirus was performed with the same

series of primers using genomic DNA from the patients' peripheral blood mononuclear cells (PBMCs) as template. The origin of the sequence (viral RNA or proviral DNA) is indicated in Table 1. PCR products were excised from preparative gels, purified by QiaQuick columns, sequenced using the inner PCR primers from both directions and aligned using ClustalW; ambiguities were resolved by direct analysis of sequencing scans using a sequence alignment editor BioEdit [22].

The p26 sequences were monitored to rule out cross-contamination during sample handling or PCR. Contamination among different samples would generate multiple sequences with 100% identity. A phylogenetic analysis showed no identical sequences, with the closest pairs (CO336 and CO335) showing 0.58% difference (4 differences in 690 nucleotides). BLAST analyses revealed no homology greater than 94% with any sequence in the GenBank database (results not shown). All the p26 sequences were consistent with HIV-2 subtype A infections.

2.3. HIV-2 envelope gene amplification

Envelope sequences were obtained from 34 HIV-2 isolates selected randomly from the set of 69 Caio viruses (see below). The following PCR primers targeted to conserved envelope flanking sequences were used:

MO080 (outer forward) CAGTCATCACAGAGTCATGTG
MO076 (outer reverse) TCCTTGTGGATAYGAYCTGT
MO072 (inner forward) TCATGTGAYAAGCACTATTGGGA
MO077 (inner reverse) GGAAGAGAAAACAGGCCTATAGCC.

An approximately 1500 bp fragment (HIV-2_{ROD} C2 to gp41, positions 6783–8285) was amplified in a nested RT-PCR from plasma virus. PCR products were purified as described above, sequenced using inner PCR primers from both directions. If the initial four primers failed, these additional primers were used:

MO122a GTGGACTAACTGCAGAGGAGAATT
MO125 AGTTCTGCCACCTCTGCACT
MO125a AGAAAACCCAAGAACCCTAGCAC.

A fragment of approximately 1300 bp corresponding to HIV-2_{ROD} positions 6849–8210 was used for the phylogenetic analysis. The p26 and Env sequences described in this manuscript were submitted to GenBank (accession numbers GQ485448-GQ485550).

2.4. Molecular modelling

Three-dimensional (3-D) models of HIV-2 CAs were constructed by the homology-modelling technique using the Molecular Operating Environment (MOE) (Chemical Computing Group Inc., Quebec, Canada) as described in Refs. [23–26]. The two crystal structures of the HIV-1 CA proteins were used as templates for the modelling; a CA monomer at a resolution of 3.00 Å (Protein Data Bank (PDB) code: 1E6J [27]) and the dimer of CA C-terminal domain at a resolution of 1.70 Å (PDB code: 1A8O [19]). The amino acid sequence identity of HIV-1 (1E6J) and HIV-2 CA (CO310 in this study) is about 70.5%. The sequence similarity is sufficient to construct a structural model with an r.m.s. deviation of approximately 1.5 Å for the main chain between the predicted and actual structures [28]. The 3-D structures were optimized thermodynamically by energy minimization using MOE and an AMBER99 force field [29] and further refined the physically unacceptable local structures on the basis of evaluation of unusual dihedral angles, ψ and ϕ, by the Ramachandran plot using MOE.

The binding energies of the p26 dimer models, E_{bind}, were calculated as described elsewhere [25] [30], using the formula $E_{bind} = E_{dimer} - 2E_{monomer}$, where E_{dimer} is the energy of the p26 dimer; $E_{monomer}$ is the energy of the p26 monomer. Spearman's rank correlation coefficient for viral load and capsid binding energy and its statistical evaluation were calculated by SPSS ver 14 (SPSS Inc, Chicago).

2.5. Expression of TRIM5α

Construction of recombinant Sendai viruses (SeVs) carrying human MT4-TRIM5α-tag (Hu-TRIM5α-Sev) and cynomolgus monkey TRIM5α lacking the SPRY domain (CM-SPRY(-)-Sev) was described previously [23].

2.6. Construction of HIV-2 GH123 capsid variants

Mutant DNA constructs of infectious molecular clones of HIV-2 GH123 carrying alanine 119 (GH123/119A) was described previously [23]. Note that because of an insertion in the GH123 p26 protein, positions 120, 160 and 179 from Ref. [23] correspond to positions 119, 159 and 178 in this work. PCR-based mutagenesis with primer pairs P1, P2 and P3, P4 was used to generate mutant GH123 carrying alanine 178 (GH123/178A). Mutant GH123 carrying serine 159 and 178A (GH123/159S-178A) was then constructed using primer pairs P1, P5 and P4, P6 with GH123/178A as a template. Mutant GH123 carrying 119A, 159S and 178A (GH123/119A-159S-178A) was constructed with primer pairs P1, P5 and P4, P6; and both GH123/119A and GH123/178A as templates. Infectious viruses were prepared by transfection of 293T cells with mutant proviral DNA clones.

P1:CTTCCCTGTACAACAGACA, P2:TTTACTGCTGCATCTGTTTGTTCTG,
P3:CAGAACAAACAGATGCAGCAGTAAA,
P4:GTGCAGCAAGTCCTCTGTC
P5:TAGCTCTGGAATGATTCCTTTGGTCC,
P6:GGACCAAAGGAATCATTCCAGAGCTA

3. Results

3.1. p26 CA variation in the Caio cohort.

HIV-2 positive subjects were selected from the Caio community cohort to assess HIV-2 sequence variation among a wide range of VL (≤100 to >280,000 copies/ml). PCR was attempted from a total of 92 subjects and p26 sequences were obtained from 69 subjects; 53 sequences were derived from viral RNA and 16 were from proviral DNA. Additional clinical features of these patients were previously described [14].

Caio p26 sequences were compared to either the Caio 69 p26 consensus sequence (Fig. 1 upper) or to the reference strain HIV-2_{ROD} p26 [31] (Fig. 1 lower) to identify amino acid polymorphisms in p26. HIV-2_{ROD} was chosen as a reference because the virus was isolated early in the epidemic in Cape Verde, islands historically linked to Guinea Bissau. Both comparisons show a similar pattern with variant amino acid sites clustering outside of the alpha helices (marked in black) required for CA folding (Fig. 1). Variations that associate with high or low VL (Mann–Whitney test, $p < 0.05$, except for position 178) are highlighted with a dotted line. The polymorphisms at position 119, 159 and 178 were of special interest because they showed 35–70% variation from HIV-2_{ROD} and involved changes from the reference sequence proline, a change expected to strongly alter protein structure. The non-proline residues were either alanine (38 cases), glutamine (5), or glycine (1) at position 119, serine (29) or threonine (2) at 159, and alanine (18), serine (2), gultamine (1), or valine (1) at 178. Viruses in low VL patients often had proline at these three positions while in higher VL samples these sites were frequently occupied by

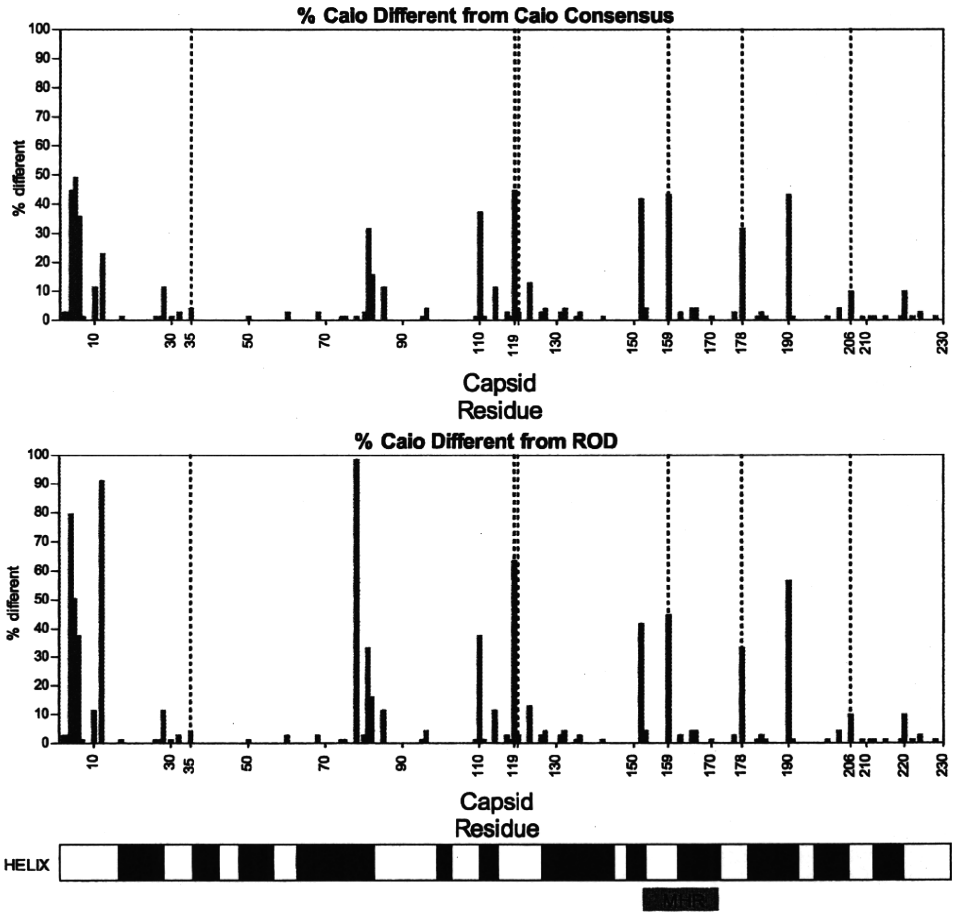

Fig. 1. Amino acid polymorphisms in the Caio HIV-2 p26. Polymorphisms in the p26 coding sequence are displayed as the percentage of the 69 sequences that differ at each position from either the Caio p26 consensus sequence (determined as the majority amino acid at each position, upper panel) or from the HIV-2_{ROD} p26 sequence (middle panel). Conserved alpha helices (in black) and the Major Homology Region (MHR) are indicated in the lower panel. Sites of variation that were associated with VL are indicated with dotted lines (Mann–Whitney test) ($p \leq 0.05$). [NB $p = 0.07$ for P178].

non-proine residues (Table 1). Three of the significantly varying positions (35, 120 and 206) were too infrequent for further study.

3.2. p26 CA variation correlating with VL

The association of proline 119, 159 and 178 with reduced VL becomes apparent when the log-transformed VL for each sample is plotted as a function of the total number of prolines at these three sites Fig. 2A. A Tobit regression analysis showed a clear relationship of increased VL with decreasing prolines in these three positions ($p = 0.003$).

To examine proline variation in more detail, CA types were grouped according the residue at each of the three positions using the code P (proline), N (not proline), or the wild card * (any amino acid) and ordered by increasing VL (Fig. 2B). Among the progression of median viral loads, there was a pattern of decreasing prolines, starting with the PPP group, through the intermediate forms to the complete non-proline NNN group (Fig. 2B). The two exceptions to this trend (the single proline NPN group had a lower median VL than the PNP and NPP groups) indicated that there may be interactions between specific combinations of these prolines in their effects on viral load but the number of examples was too small to demonstrate such effects statistically.

Considering the effect of single proline changes, proline 119 (P119) CAs (the P group) were isolated more frequently from patients with low VL with a 4.9-fold difference in the median VL of P** group compared to the N** group ($p = 0.0205$; Fig. 2B).

Proline 159 (P159) had a stronger effect on VL with at least 6.1-fold difference in the median VL of the *P* group compared to the *N* group ($p = 0.0075$; Fig. 2B). This site is of special interest being within the highly conserved MHR (Fig. 1) [20], essential for virion assembly.

Proline 178 (P178) showed modest variation with VL with only 3.5-fold difference in the median VL of the **P group compared to the **N group ($p = 0.0709$; Fig. 2B,). However, the presence of P178 was linked to the other two prolines: all CAs with both P119 and P159 had P178 (i.e. the PPP group = the PP* group, Fig. 2B). This may be due to a p26 folding requirement and/or genetic linkage.

Stronger associations were observed when the positions were analyzed in combination. The median VL in subjects with PP* viruses differed from NN* viruses by at least 13.6-fold ($p = 0.0028$, Fig. 2B). Importantly, median VL in subjects with viruses having all three prolines (PPP) compared to those lacking a proline at the sites (NNN) differed by at least 18.8-fold ($p = 0.0013$, Fig. 2B).

There are practical difficulties of sequencing circulating RNA genomes, especially from patients with <100 copies viral RNA per ml of plasma. Sixteen of the 69 sequences were derived from proviral DNA (listed as DNA in Table 1) because multiple attempts to obtain RNA sequence failed. To test if proline/VL associations were biased by the inclusion of these proviral sequences, the analysis was repeated after excluding the data from these 16 samples. The association of higher VL with non-proline residues remained significant at positions 119 ($p = 0.0123$) and 159 ($p = 0.0043$), and for the combined positions 119+159 ($p = 0.0012$) and 119+159+178

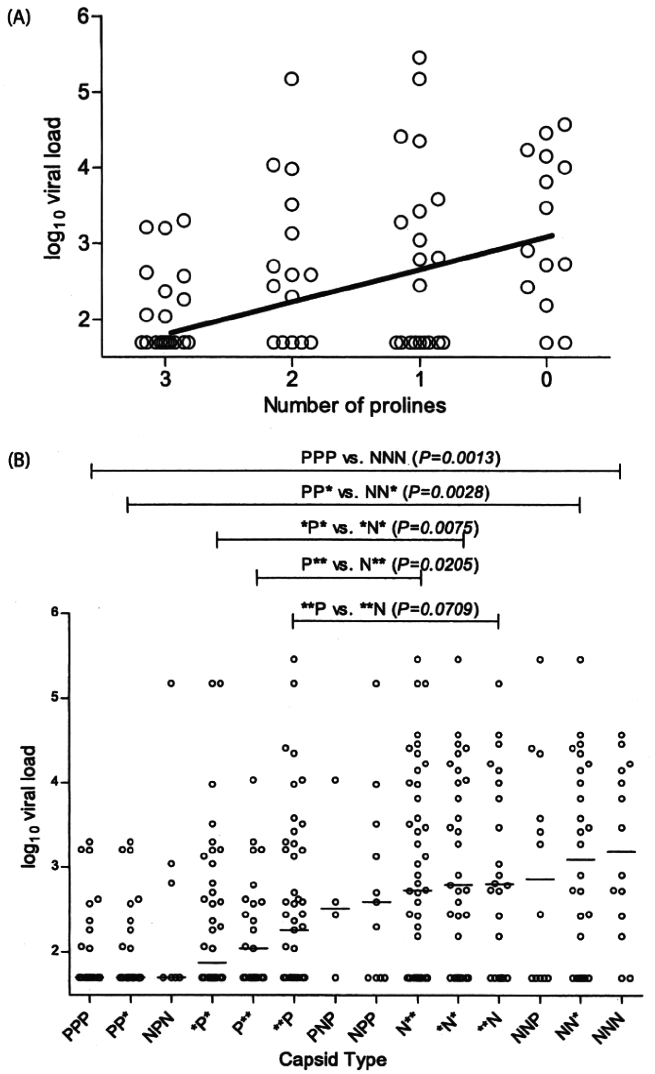

Fig. 2. HIV-2 VL correlates with amino acid variation at three p26 sites. (A) Relationship between VL and the number of prolines. Log-transformed VL for each sample was plotted as a function of the total number of prolines at p26 positions 119, 159 and 178. Tobit regression (Stata10, StatCorp TX, USA) was used to investigate the relationship between VL and the number of prolines at positions 119, 159 and 178. This form of regression is able to allow for censoring of viral loads below 100 in the dataset. The regression line was drawn with the equation $\log_{10}VL = 3.15 - 0.46 \times$ No. of prolines. (B) Relationship between VL and type of PPP motif. Log-transformed VL for each sample is plotted as a function of amino acid variation at p26 position 119, 159 and 178. Median VL are indicated by horizontal bars. The patients were stratified by the presence of proline (P) no proline residue (N) or any amino acid (*) at each of the positions 119, 159 and 178. For example, PPP = proline resides at positions 119, 159 and 178, NNN = no proline at the three positions. Comparisons of plasma VLs for different amino acid polymorphisms of particular interest were made using the non-parametric Mann–Whitney test (GraphPad Prism 5). *p*-values for these are shown above the figure.

($p = 0.0024$) (Table S1, lower panel). We conclude that independent of the origin of the sequences, there exists an association between low VL and proline residues at positions 119 and 159 independently, and with 119, 159 and 178 combined.

3.3. p26 CA variation influences susceptibility to TRIM5α

The TRIM5α was identified as a limit to cross-species retroviral infection [32–35]. This has led to a model of TRIM5α blocking retroviral infection by binding to the CA during entry, accelerating virus uncoating, and limiting subsequent steps in the infection process [32,34,36,37]. P119 was recently identified as a determinant of TRIM5α restriction [23] with HIV-2 CAs derived from TRIM5α sensitive viruses bearing a proline, and resistant strains having an alanine or glutamine at this site. It is possible that the reduced replication of the PPP viruses we observed in patients was part of the same phenomenon. Accordingly, the contribution of all three proline residues to TRIM5α restriction of replication was directly examined *in vitro*. Starting with the HIV-2 strain GH-123 as a PPP virus, P119, P159 plus P178, or all three prolines were altered to alanine or serine using site-directed mutagenesis. The growth of these variant viruses was compared in cells modified to express human TRIM5α; a parallel cell line expressing TRIM5α missing the SPRY domain, essential for p26 interaction, was used as a control to determine if these p26 changes altered virus replication independent of TRIM5α function [23]. Altering P119 (to produce APP) or P159 + P178 (to produce PSA) allowed 3-fold greater virus replication Fig. 3A. Alteration of all three prolines to ASA resulted in a 6-fold increase in virus replication. Thus the GH-123 variants displayed replication *in vitro* that closely mimic the behavior of the HIV-2 variants *in vivo*.

3.4. Phylogenetic analysis of p26 CA variation

One possible origin of the PPP form of p26 is that such a CA was encoded by a founder variant of HIV-2. The reduced growth of PPP viruses could be due to the p26 itself or to other shared and co-evolved features in these viruses. Alternately, changes at these three codons could occur more frequently. A phylogenetic analysis of Caio HIV-2 was performed to distinguish the PPP founder virus model from a multiple occurrence model. A founder effect with the appearance and spread of a PPP virus would appear as phylogenetic clustering of these variants. Ongoing selection for or against prolines in p26 would result in a phylogeny lacking PPP clustering. Because results derived from the 960 bp containing p26 coding could be dominated by variation in codons 119, 159 and 178, phylogeny was also inferred from a larger sequence spanning approximately 1300 bp of the envelope gene and including the highly variable V3 and V4 loops. The inferred phylogenies show that HIV-2 isolates encoding PPP p26 are distributed throughout the p26 and envelope trees (Fig. S1), supporting the conclusion that the occurrence of PPP p26 is not associated with a specific phylogenetic branch of Caio HIV-2 and is unlikely to be associated with a single occurrence of this CA motif. This conclusion is also supported by the high bootstrap values for some of the branches. These results are consistent with selection for and multiple appearance of the PPP p26 in the Caio population.

3.5. Modelling p26 CA sequence variation on structure and dimer formation

The bulky and constrained structure of proline strongly influences protein secondary structure; proline is inimical to alpha-helices and can kink otherwise flexible loops [38]. Thus polymorphisms involving prolines residues could alter the p26 structure. Using homology modelling, three-dimensional structures of six of the Caio HIV-2 p26 molecules (2 PPP, 2 ASA and 2 intermediate forms, APP and ASP) were constructed. The thermodynamically optimized 3-D structure models showed that the HIV-2 p26 consists of two packed core structures of N-terminal and C-terminal domains, a similar conformation to HIV-1 p24 [39]. Superimposition of the six HIV-2 p26 models showed that the overall 3-D structures of the variants were very similar with an exception: the amino acid substitution at position 119 from proline to alanine induced marked changes in the configuration of the loop between helices 6 and 7, as found previously with HIV-2 p26 N-terminal domain model [23]. In contrast, the substitution

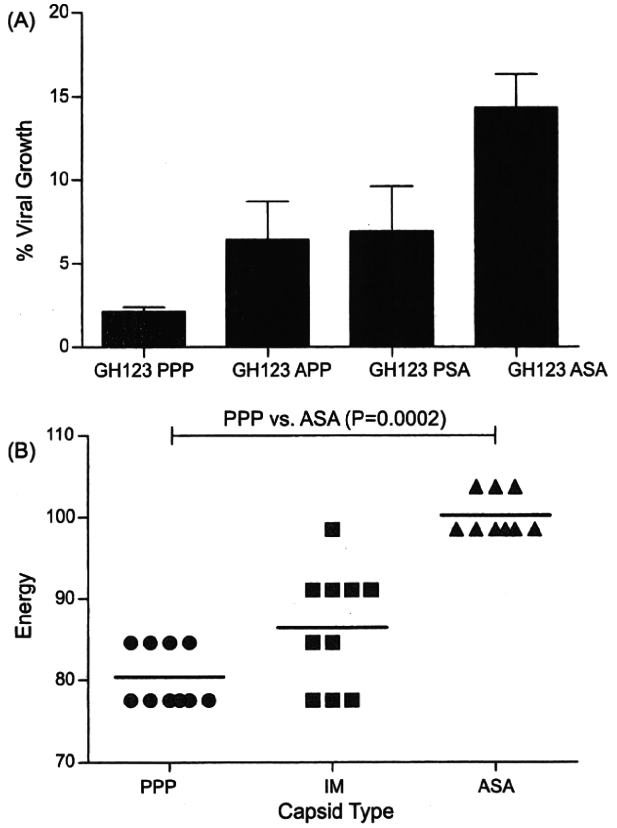

Fig. 3. HIV-2 capsid changes alter TRIM5α susceptibility and capsid stability. (A) Growth of HIV-2 GH123 (PPP) and its mutant viruses HIV-2 GH123/119A (APP), HIV-2 GH123/159S-178A (PSA), and HIV-2 GH123/119A-159S-178A (ASA) in the presence of human TRIM5α. MT4 cells (10^5) were infected with Hu-TRIM5α-SeV or CM-SPRY(-)-SeV at a multiplicity of infection of 10 plaque forming units per cell. 9 h after infection, the cells were superinfected with 20 ng of p26 of HIV-2 GH123, HIV-2 GH123/119A, HIV-2 GH123/159S-178A, or HIV-2 GH123/119A-159S-178A viruses. The culture supernatants were collected 6 days after infection, and the level of p26 was measured by using a RETROtek antigen ELISA kit (ZeptoMetrix Corp., Buffalo, NY). Ratios of HIV-2 CA levels of Hu-TRIM5α-SeV-infected cells to those of CM-SPRY(-)-SeV-infected cells are shown as percent growth. Error bars denote standard deviations in quadruplicate samples. A Kruskal–Wallis test for the entire data set clearly detected the difference of viral growth among those four viruses ($p = 0.006$). Furthermore, comparison of each mutant virus with GH123(PPP) using the Dunnett test also showed statistically significant differences of PPP vs. APP $p < 0.05$, PPP vs. PSA $p < 0.05$, and PPP vs. ASA $p < 0.01$. (B) Dimer binding energies as a function of capsid type. Samples were grouped into PPP, IM (intermediate, with proline at one or two of the three sites) or ASA, based on the amino acid at position 119, 159 and 178. The capsid dimer binding energies (absolute value) for each sequence were determined by homology modelling (see Section 2); the mean values for each group are indicated. Comparison between the PPP and the ASA group using the non-parametric Mann–Whitney test (GraphPad Prism 5) provided the indicated p-value.

at positions 159 or 178 induced no major changes in the main-chain backbone of HIV-2 CA (data not shown), suggesting that the structure of the CA can accommodate alternative residues at these sites.

Positions 159 and 178 are located in the C-terminal portion of p26 required for dimer formation as well as virion shell assembly [18]. Homology modelling of the p26 dimer was used to calculate binding energy for dimer formation. Since the C-terminal sequences used to prepare the initial six structures were common to a larger set of p26 sequences, dimer binding energies for 29 of the Caio CAs could be calculated. These calculations revealed that the PPP p26 dimers had weaker binding energies, the ASA dimers had stronger binding energies and the intermediate forms with only one or two of the prolines altered (IM) had intermediate binding energies (Fig. 3B). In addition, the viral loads of the 29 patients were modestly correlated with the absolute values of the binding energy of the viral CA ($r_s = 0.383$, $p = 0.040$). We conclude that the amino acid changes at positions 159 and 178 influence p26 dimer stability, with ASA CA dimers having a higher stability than PPP or APP CA dimers and the increased stability may be related to elevated VL in these patients.

4. Discussion

This study represents a detailed examination of HIV-2 p26 sequence variation within a set of 69 sequences isolated from subjects with both high and low VL. Disease progression after HIV-2 infection is highly dependent on VL [40] with subjects who control HIV-2 replication continuing to do this over a period of many years, suggesting that virus-host interactions result in a stable set-point of virus replication. The current study identified three sites of p26 variation correlating with VL. This study reveals a previously undescribed pattern of variation in the highly conserved p26 and indicates that the outcome of HIV-2 infection is partially predicted by the form of the p26 carried by the virus. In addition to confirming the importance of P119 as a determinant of TRIM5α restriction, the current study identified two additional amino acid positions (159 and 178) whose identities correlate with virus load. Although these associations were not significant after stringent adjustment for multiple comparisons, HIV-2 encoding p26 specifically modified at these three positions showed *in vitro* replication levels consistent with the *in vivo* VL data and further supported the conclusion that the three residues 119, 159 and 178 are important determinants of virus growth and influence TRIM5α restriction (Fig. 3).

Virus replication *in vivo* is influenced by a large number of host and viral factors and it would be naïve to conclude that these three residues are the sole determinants. That additional factors influence the course of infection is reflected in the VL data and the exceptions from the pattern (e.g. the three PPP viruses with greater than 10e3 VL and the 2 NNN viruses with undetectable VL). However, the power of such a population study is that patterns of HIV-2 behavior appear when large numbers of infection are monitored. As shown in Fig. 2, the substantial and statistically significant change in VL that accompanies the variation from PPP to NNN viruses strongly supports our conclusions that this p26 motif is an important determinant of the course of infection.

How might the PPP motif function? Our data support a destabilization of the CA by the three proline residues. P119 may directly form a recognition signal for TRIM5α binding, and the three proline residues may result in less tightly packed core that is more readily dismantled and processed after TRIM5α recognition. Our preliminary immunological studies show that patients with PPP virus mount stronger T cell responses to p26 and to the entire HIV-2 proteome (A.L., S.R.J. unpublished results) and this increased immune exposure might be a consequence of TRIM5α recognition and more efficient antigen presentation.

These results are consistent with TRIM5α restriction playing a direct role in limiting HIV-2 replication and a more indirect role in enhancing the immune response to the virus. The *in vitro* studies (Fig. 3A), although using manipulated cells and monitoring virus replication only over a short period of replication, demonstrated that variation in these three CA residues influence the susceptibility of HIV-2 replication to TRIM5α. *In vivo*, it is likely that TRIM5α effects are both manifested over multiple rounds of infection and TRIM5α may cooperate with other processes such as the adaptive immune response; *in vitro* cell culture conditions and growth in immortalized cell lines are unlikely to fully recreate these processes. We believe that our *in vivo* virus load data are the strongest support for the hypothesis that the PPP motif modulates VL.

If our hypothesis is correct, incident infections in Caio, infected patients that progress to require anti-retroviral therapy and moth-

ers who infected their children should have a marked abundance of non-PPP forms. In fact, our phylogenetic analysis demonstrated no PPP virus clusters while there are some clusters of non-PPP viruses (Fig. S1), suggesting more frequent transmission of non-PPP viruses than PPP virus. We are currently examining these possibilities.

If the PPP p26 molecule is associated with a number of fitness-decreasing properties, what maintains this less fit gene in the population? One possibility is that there may be direct HLA selection for proline residues at these p26 positions. All three proline sites lie within or adjacent to known HLA epitopes. The presence of these key proline residues could either block the host immune recognition of these epitopes or interfere with processing to release the epitope. HIV-1 clearly adapts to its current host's HLA system by changing recognized epitopes [41–45] and it is likely that HIV-2 is subject to the same host HLA selection. Thus virus evolution may be driven by a shortsighted response to HLA selection resulting in PPP p26 that in the long term results in reduced viral replication. An abundance of HLA alleles in Caio that select for PPP p26 may be responsible for the high frequency of controlled HIV-2 infections in Caio. A cross-sectional study on HLA associations with p26 variation is underway. Adaptation to the current host's HLA haplotype has important consequences for the design of T cell based vaccines and could be exploited in vaccines to encourage the evolution of less aggressive variants.

Acknowledgements

Contributors: John Townend provided statistical expertise. We appreciate the help and support of Ramu Sarge-Njie for providing serological data and Abraham Alabi for providing viral load data for these studies. We thank Tim Vincent and the staff of the Caio field station for facilitating the field work and Carla van Tienen, Bouke DeJong and Neil Berry for critical reading of the manuscript.

Appendix A. Supplementary data

Supplementary data associated with this article can be found, in the online version, at doi:10.1016/j.vaccine.2009.08.060.

Conflict of interest statement

The authors state that they have no conflict of interest.

References

[1] Barin F, M'Boup S, Denis F, Kanki P, Allan JS, Lee TH, et al. Serological evidence for virus related to simian T-lymphotropic retrovirus III in residents of west Africa. Lancet 1985;2(8469–70):1387–9.
[2] Clavel F, Guetard D, Brun-Vezinet F, Chamaret S, Rey MA, Santos-Ferreira MO, et al. Isolation of a new human retrovirus from West African patients with AIDS. Science 1986;233(4761):343–6.
[3] Lemey P, Pybus OG, Wang B, Saksena NK, Salemi M, Vandamme AM. Tracing the origin and history of the HIV-2 epidemic. Proc Natl Acad Sci USA 2003;100(11):6588–92.
[4] Rowland-Jones SL, Whittle HC. Out of Africa: what can we learn from HIV-2 about protective immunity to HIV-1? Nat Immunol 2007;8(4):329–31.
[5] Poulsen AG, Kvinesdal B, Aaby P, Molbak K, Frederiksen K, Dias F, et al. Prevalence of and mortality from human immunodeficiency virus type 2 in Bissau, West Africa. Lancet 1989;1(8642):827–31.
[6] Berry N, Ariyoshi K, Balfe P, Tedder R, Whittle H. Sequence specificity of the human immunodeficiency virus type 2 (hiv-2) long terminal repeat u3 region in vivo allows subtyping of the principal hiv-2 viral subtypes a and b. AIDS Res Hum Retroviruses 2001;17(3):263–7.
[7] Berry N, Ariyoshi K, Jaffar S, Sabally S, Corrah T, Tedder R, et al. Low peripheral blood viral HIV-2 RNA in individuals with high CD4 percentage differentiates HIV-2 from HIV-1 infection. J Hum Virol 1998;1(7):457–68.
[8] Ariyoshi K, Jaffar S, Alabi AS, Berry N, Schim van der Loeff M, Sabally S, et al. Plasma RNA viral load predicts the rate of CD4 T cell decline and death in HIV-2-infected patients in West Africa. AIDS 2000;14(4):339–44.
[9] Gao F, Yue L, Robertson DL, Hill SC, Hui H, Biggar RJ, et al. Genetic diversity of human immunodeficiency virus type 2: evidence for distinct sequence subtypes with differences in virus biology. J Virol 1994;68(11):7433–47.
[10] Ricard D, Wilkins A, N'Gum PT, Hayes R, Morgan G, Da Silva AP, et al. The effects of HIV-2 infection in a rural area of Guinea-Bissau. AIDS 1994;8(7):977–82.
[11] Grassly NC, Xiang Z, Ariyoshi K, Aaby P, Jensen H, Schim van der Loeff M, et al. Mortality among human immunodeficiency virus type 2-positive villagers in rural Guinea-Bissau is correlated with viral genotype. J Virol 1998;72(10):7895–9.
[12] Norrgren H, Marquina S, Leitner T, Aaby P, Melbye M, Poulsen AG, et al. HIV-2 genetic variation and DNA load in asymptomatic carriers and AIDS cases in Guinea-Bissau. J Acquir Immune Defic Syndr Hum Retrovirol 1997;16(1):31–8.
[13] Padua E, Jenkins A, Brown S, Bootman J, Paixao MT, Almond N, et al. Natural variation of the Nef gene in human immunodeficiency virus type 2 infections in Portugal. J Gen Virol 2003;84(Pt 5):1287–99.
[14] Leligdowicz A, Yindom LM, Onyango C, Sarge-Njie R, Alabi A, Cotten M, et al. Robust Gag-specific T cell responses characterize viremia control in HIV-2 infection. J Clin Invest 2007;117(10):3067–74.
[15] Mortuza GB, Haire LF, Stevens A, Smerdon SJ, Stoye JP, Taylor IA. High-resolution structure of a retroviral capsid hexameric amino-terminal domain. Nature 2004;431(7007):481–5.
[16] Briggs JA, Grunewald K, Glass B, Forster F, Krausslich HG, Fuller SD. The mechanism of HIV-1 core assembly: insights from three-dimensional reconstructions of authentic virions. Structure 2006;14(1):15–20.
[17] Ganser BK, Li S, Klishko VY, Finch JT, Sundquist WI. Assembly and analysis of conical models for the HIV-1 core. Science 1999;283(5398):80–3.
[18] Ganser-Pornillos BK, Yeager M, Sundquist WI. The structural biology of HIV assembly. Curr Opin Struct Biol 2008;18(2):203–17.
[19] Gamble TR, Yoo S, Vajdos FF, von Schwedler UK, Worthylake DK, Wang H, et al. Structure of the carboxyl-terminal dimerization domain of the HIV-1 capsid protein. Science 1997;278(5339):849–53.
[20] Mammano F, Ohagen A, Hoglund S, Gottlinger HG. Role of the major homology region of human immunodeficiency virus type 1 in virion morphogenesis. J Virol 1994;68(8):4927–36.
[21] Alabi AS, Jaffar S, Ariyoshi K, Blanchard T, Schim van der Loeff M, Awasana AA, et al. Plasma viral load, CD4 cell percentage, HLA and survival of HIV-1, HIV-2, and dually infected Gambian patients. AIDS 2003;17(10):1513–20.
[22] Hall TA. BioEdit: a user-friendly biological sequence alignment editor and analysis program for Windows 95/98/NT. Nucleic Acids Symp Ser 1999;41:95–8.
[23] Song H, Nakayama EE, Yokoyama M, Sato H, Levy JA, Shioda T. A single amino acid of the human immunodeficiency virus type 2 capsid affects its replication in the presence of cynomolgus monkey and human TRIM5alphas. J Virol 2007;81(13):7280–5.
[24] Kinomoto M, Yokoyama M, Sato H, Kojima A, Kurata T, Ikuta K, et al. Amino acid 36 in the human immunodeficiency virus type 1 gp41 ectodomain controls fusogenic activity: implications for the molecular mechanism of viral escape from a fusion inhibitor. J Virol 2005;79(10):5996–6004.
[25] Kinomoto M, Appiah-Opong R, Brandful JA, Yokoyama M, Nii-Trebi N, Ugly-Kwame E, et al. HIV-1 proteases from drug-naive West African patients are differentially less susceptible to protease inhibitors. Clin Infect Dis 2005;41(2):243–51.
[26] Shirakawa K, Takaori-Kondo A, Yokoyama M, Izumi T, Matsui M, Io K, et al. Phosphorylation of APOBEC3G by protein kinase A regulates its interaction with HIV-1 Vif. Nat Struct Mol Biol 2008;15(11):1184–91.
[27] Monaco-Malbet S, Berthet-Colominas C, Novelli A, Battai N, Piga N, Cheynet V, et al. Mutual conformational adaptations in antigen and antibody upon complex formation between an Fab and HIV-1 capsid protein p24. Structure 2000;8(10):1069–77.
[28] Baker D, Sali A. Protein structure prediction and structural genomics. Science 2001;294(5540):93–6.
[29] Ponder JW, Case DA. Force fields for protein simulations. Adv Protein Chem 2003;66:27–85.
[30] Lee K, Chu CK. Molecular modelling approach to understanding the mode of action of L-nucleosides as antiviral agents. Antimicrob Agents Chemother 2001;45(1):138–44.
[31] Guyader M, Emerman M, Sonigo P, Clavel F, Montagnier L, Alizon M. Genome organization and transactivation of the human immunodeficiency virus type 2. Nature 1987;326(6114):662–9.
[32] Stremlau M, Owens CM, Perron MJ, Kiessling M, Autissier P, Sodroski J. The cytoplasmic body component TRIM5alpha restricts HIV-1 infection in old World monkeys. Nature 2004;427(6977):848–53.
[33] Goff SP. HIV: replication trimmed back. Nature 2004;427(6977):791–3.
[34] Towers G, Bock M, Martin S, Takeuchi Y, Stoye JP, Danos O. A conserved mechanism of retrovirus restriction in mammals. Proc Natl Acad Sci USA 2000;97(22):12295–9.
[35] Stremlau M. GE Prize-winning essay, Why old World monkeys are resistant to HIV-1. Science 2007;318(5856):1565–6.
[36] Cowan S, Hatziioannou T, Cunningham T, Muesing MA, Gottlinger HG, Bieniasz PD. Cellular inhibitors with Fv1-like activity restrict human and simian immunodeficiency virus tropism. Proc Natl Acad Sci USA 2002;99(18):11914–9.
[37] Stremlau M, Perron M, Lee M, Li Y, Song B, Javanbakht H, et al. Specific recognition and accelerated uncoating of retroviral capsids by the TRIM5alpha restriction factor. Proc Natl Acad Sci USA 2006;103(14):5514–9.
[38] Creighton TE. Proteins: Structures and Molecular Properties. 2nd ed. New York: W.H. Freeman; 1992.
[39] Howard BR, Vajdos FF, Li S, Sundquist WI, Hill CP. Structural insights into the catalytic mechanism of cyclophilin A. Nat Struct Biol 2003;10(6):475–81.

[40] Berry N, Jaffar S, Schim van der Loeff M, Ariyoshi K, Harding E, N'Gom PT, et al. Low level viremia and high CD4% predict normal survival in a cohort of HIV type-2-infected villagers. AIDS Res Hum Retroviruses 2002;18(16):1167–73.
[41] Moore CB, John M, James IR, Christiansen FT, Witt CS, Mallal SA. Evidence of HIV-1 adaptation to HLA-restricted immune responses at a population level. Science 2002;296(5572):1439–43.
[42] Brumme ZL, Tao I, Szeto S, Brumme CJ, Carlson JM, Chan D, et al. Human leukocyte antigen-specific polymorphisms in HIV-1 Gag and their association with viral load in chronic untreated infection. AIDS 2008;22(11):1277–86.
[43] Bhattacharya T, Daniels M, Heckerman D, Foley B, Frahm N, Kadie C, et al. Founder effects in the assessment of HIV polymorphisms and HLA allele associations. Science 2007;315(5818):1583–6.
[44] Kawashima Y, Pfafferott K, Frater J, Matthews P, Payne R, Addo M, et al. Adaptation of HIV-1 to human leukocyte antigen class I. Nature 2009;458(7238):641–5.
[45] Klenerman P, McMichael A. AIDS/HIV. Finding footprints among the trees. Science 2007;315(5818):1505–7.
[46] Kimura M. A simple method for estimating evolutionary rates of base substitutions through comparative studies of nucleotide sequences. J Mol Evol 1980;16(2):111–20.
[47] Tamura K, Dudley J, Nei M, Kumar S. MEGA4: molecular evolutionary genetics analysis (MEGA) software version 4.0. Mol Biol Evol 2007;24(8):1596–9.
[48] Saitou N, Nei M. The neighbor-joining method: a new method for reconstructing phylogenetic trees. Mol Biol Evol 1987;4(4):406–25.
[49] Tamura K, Nei M, Kumar S. Prospects for inferring very large phylogenies by using the neighbour-joining method. Proc Natl Acad Sci USA 2004;101(30):11030–5.
[50] Wilkins A, Ricard D, Todd J, Whittle H, Dias F, Paulo Da Silva A. The epidemiology of HIV infection in a rural area of Guinea-Bissau. AIDS 1993;7(8):1119–22.

TIM1 haplotype may control the disease progression to AIDS in a HIV-1-infected female cohort in Thailand

Nuanjun Wichukchinda[a,1], Toshiaki Nakajima[b,1], Nongluk Saipradit[a], Emi E. Nakayama[c], Hitoshi Ohtani[b], Archawin Rojanawiwat[a], Panita Pathipvanich[d], Koya Ariyoshi[e], Pathom Sawanpanyalert[a], Tatsuo Shioda[c,1] and Akinori Kimura[b,1]

Objective: To investigate association of TIM1 sequence variations with HIV/AIDS progression.

Introduction: HIV-1 infected individuals have wide variations in disease progression including AIDS. T cell immunoglobulin and mucin 1 (TIM1) is a cell surface protein involved in the regulation of Th1/Th2 immune response.

Materials and methods: We sequenced the highly polymorphic exon 4 of *TIM1* from 246 individuals of HIV-1 infected Thai female cohort to determine their *TIM1* haplotypes. Associations of *TIM1* haplotypes with baseline clinical data (sero-status, plasma viral load, CD4 cell count, and symptomatic AIDS) and survival status during 3 years of follow-up were evaluated.

Results: Seven *TIM1* haplotypes, D3-A, D4, D3-C, D1, W-A, W-C, and D3-C*, were found in the cohort. Patients possessing the D3-A haplotype showed trends towards higher $CD4^+$ cell count ($P=0.06$) and lower proportion of AIDS-related symptoms ($P=0.022$) than the other patients at the baseline. Kaplan–Meier analysis demonstrated that patients carrying the D3-A haplotype had a better survival rates ($P=0.019$) than the others. D3-A haplotypes was tightly linked to the lower expression levels of *TIM1*.

Conclusion: *TIM1* D3-A haplotype is associated with the delay of disease progression to AIDS in the HIV-1 infected Thai females.

AIDS 2010, **24**:1625–1631

Keywords: disease progression, HIV-1, polymorphism, survival rate, TIM1

Introduction

T-cell immunoglobulin (Ig) and mucin domain (TIM) proteins, which expressed on T cells, play a central role in regulating Th1-cell and Th2-cell mediated immune response [1,2]. The genes for human TIM proteins are located on chromosome 5q31-33 and include three members; *TIM1*, *TIM3*, and *TIM4*. *TIM1* is called a hepatitis A cellular receptor 1 (*HAVCR1*) because it was originally identified as a receptor for hepatitis A virus [3]. *TIM1* is also known as kidney injury molecule 1 (*KIM1*) [4] and encodes for 359-amino acid membrane protein containing a putative signal sequence (residues 1–20), Ig domain (residues 21–121), mucin domain (residues 130–205), transmembrane (residues 291–311), and 50-amino acid long cytoplasmic tail [5].

[a]National institute of Health, Department of Medical Sciences, Ministry of Public Health, Nonthaburi, Thailand, [b]Department of Molecular Pathogenesis, Medical Research Institute, and Laboratory of Genome Diversity, Graduate School of Biomedical Science, Tokyo Medical and Dental University, Tokyo, [c]Department of Viral Infections, Research Institute for Microbial Diseases, Osaka University, Osaka, Japan, [d]Day Care Center, Lampang Hospital, Lampang, Thailand, and [e]Global COE Program and Department of Clinical Medicine, Institute of Tropical Medicine, Nagasaki University, Nagasaki, Japan.

Correspondence to Akinori Kimura, Department of Molecular Pathogenesis, Medical Research Institute, Tokyo Medical and Dental University, 1-5-45 Yushima, Bunkyo-ku, Tokyo 113-8510, Japan.

Tel: +81 3 5803 4905; fax: +81 3 5803 4907; e-mail: akitis@mri.tmd.ac.jp

[1] These authors equally contributed to this study.

Received: 15 November 2009; revised: 8 February 2010; accepted: 16 February 2010.

DOI:10.1097/QAD.0b013e32833a8e6d

TIM1 is associated with Th2 type immune responses and selectively expressed on Th2 cell [1,6]. Human *TIM1* exhibits a high degree of amino-acid variability in the extracellular mucin domain encoded by exon 4 [7]. Because mucin domain is involved in the recognition of molecules outside the cells, it was suggested that *TIM1* might have been under the selective pressure in the course of human evolution, and the variation in this gene might be involved in the difference in the susceptibility to immune-related diseases including infectious and autoimmune diseases. There are several reports on the association of polymorphisms in *TIM1* with allergic diseases [8–12]. In addition, Nuchnoi *et al.* [13] have recently reported that a *TIM1* promoter haplotype, which was linked to higher expression of *TIM1*, was associated with the resistance to cerebral malaria in Thais.

HIV-1 infection is characterized by its chronic disease course, in which $CD4^+$ T cells gradually decrease that is followed by the dysfunction of host immune system. During the course of HIV-infection, the balance between Th1 and Th2 immune responses played a crucial role in the control of viral replication [14,15]. Therefore, it is highly possible that polymorphisms of genes involved in the Th1 and Th2 immune responses potentially contribute to the disease progression to AIDS and/or the susceptibility to HIV-1 infection.

In this study, we investigated the association of *TIM1* polymorphisms with the disease progression of HIV/AIDS in 246 HIV-1-infected Thai females. It was found that the *TIM1* haplotype D3-A significantly delayed the progression to AIDS.

Materials and method

Individuals

We investigated a cohort composed of 246 HIV-1-infected women obtained from the HIV clinic in the Day Care Center of Lampang Hospital in north Thailand between July 6, 2000 and July 12, 2001 as described previously [16]. They were recruited when they visited the clinic. Although the dates of HIV infection and seroconversion were not assessed or estimated for the individuals, they were free from antiretroviral drug at the time of recruitment. We also investigated 74 exposed seronegative (ESN) Thai women [17]. For a control group, we collected blood samples from 119 female blood donors at the blood bank of the same hospital. EDTA-blood was taken from each individual at the time of recruitment, and separated for plasma and pack red cell. Plasma HIV-1 RNA copy number was measured by using a commercially available kit (Amplicor HIV-1 Monitor Test; Roche Molecular System, Inc. Branchburg, New Jersey, USA), which had a lower limit of detection at 400 copies/ml. $CD4^+$ cell count was measured by using FACScan (BD Biosciences, California, USA). The survival status of participants until 1 October 2003 was ascertained from the cohort database, mailing letters, and death certificates at the Lampang Provincial Health Office. Data were double entered and validated using the access program. This study was approved by the Ethical Review Committee for Research in Human individuals, Ministry of Public Health, Thailand in January 2000.

Genotyping

Genomic DNA was extracted and purified from the frozen buffy coat by using QIAamp DNA Blood Mini kit (QIAGEN GmbH, Hiden, Germany). Each sample was analyzed for polymorphisms in the *TIM1*-exon 4 by direct sequencing. The primer pair, forward 5′-GGGCAATGACCAAGATTGAC-3′ and reverse 5′-ACCTTGATACAATGCCCTGG-3′, was used to amplify the 470-bp fragment of *TIM1*-exon 4 by polymerase chain reaction (PCR) that was performed in a total volume of 25 μl containing 20–50 ng of genomic DNA, 100 nmol/l of each dNTPs, 0.2 μmol/l of each primer, 2.5 mmol/l of $MgCl_2$, and 0.5 U of Taq DNA polymerase (Immolase DNA polymerase; Bioline USA, Inc. Massachusetts, USA). Amplification profile included initial incubation at 94°C for 5 min, 30 cycles of 94°C for 30 s, 55°C for 30 s and 72°C for 30 s, followed by a final extension at 72°C for 5 min. The PCR products were purified by sephadex gel centrifugation, and 1 μl of purified product was then used as a template for sequencing using BigDye Terminator v 3.1 cycle sequencing kit (Applied Biosystems, Foster City, California, USA) in a total volume of 10 μl containing the PCR forward primer. Sequence analysis was done by ABI Prism 3100 Genetic Analyzer and SeqScape software version 2.5 (Applied Biosystems). Determination of *TIM1* haplotypes was base on the previous report [7]. Because there were four common insertion/deletion polymorphisms in *TIM1*-exon 4, each pattern of heterozygous samples was also analyzed by cloning the PCR product into a plasmid vector (TOPO™ TA Cloning Kit; Invitrogen, Carlsbad, California, USA) according to the manufacturer's instruction and six colonies of each sample were sequenced to further determine the *TIM1* haplotypes.

Quantification of *TIM1* transcript in human B lymphoblastoid cell lines

Human B lymphoblastoid cell lines were cultured in RPMI medium 1640 supplemented with 10% fetal bovine serum under 5% CO_2. Cells were collected at growing phase and approximately 10^7 cells were subjected to total cellular RNA preparation by RNeasy mini kit (Qiagen). One microgram of RNA was used to synthesize cDNA by Superscript II reverse transcriptase (Invitrogen) according to the manufacturer's instruction. Quantitative real-time PCR used iCycler iQ Real-Time PCR Detection System (Bio-Rad) and iQ SYBR Green Supermix kit (Bio-Rad) to measure relative amount of

mRNA by cycle threshold. Expression level of *TIM1* was normalized by the expression level of *GAPDH* and the ratio of *TIM1/GAPDH* was arbitrarily expressed as arbitrary unit (AU) for comparison of the expression levels in different cell lines. Primers and probe for quantification of *TIM1* and *GAPDH* transcripts are as follows *TIM1* sense primer 5′-CCACCAGCTCACCA TTGTACT-3′; antisense primer 5′-TCTGCTTGGA CTTCCTTTTCA-3′. *GAPDH* primer sequences are as follows sense primer 5′-CTTCACCACCATGGAGA AGGC-3′; antisense 5′-GGCATGGACTGTGGTCAT GAG-3′. Relative expression level was expressed arbitrarily as the ratio of *TIM1/GAPDH*.

Statistical analysis

Association of *TIM1* haplotype with the disease progression was assessed with respect to baseline clinical data including plasma viral load, CD4 cell count, proportion of symptomatic AIDS, and survival status during the follow-up period for 3 years. Continuous variables of two groups with different genetic background were compared by a two-tailed nonparametric Kruskal–Wallis test. Qualitative variables of two groups were compared by a chi-squared test, and the statistical significance was not corrected for multiple testing. Significance in Kaplan–Meier analysis was assessed by a log-rank test. Statistical analyses were carried out using Epi Info version 3.01 (US-CDC). Crude and adjusted hazard (HR) and their 95% confidence intervals (CI) were calculated by Cox proportional hazard models using StatView (SAS Institute Inc., Cary, North Carolina, USA). For adjustment of CD4 cell count, patients were categorized into three groups, namely, those with CD4 cell count (cells/μl) below 50, those with 50–199, and those with 200 and over.

Result

TIM1-exon 4 haplotype distribution in Thais

We previously reported a total of eleven *TIM1* haplotypes in various ethnic groups [7]. In the present study, six out of the 11 *TIM1* haplotypes were found in the studied Thai population that was composed of 246 antiretroviral drug-free HIV-positives, 74 ESNs, and 119 controls, with the most prevalent haplotype D3-A (Table 1). In addition, we found a novel haplotype (D3-C*) in one individual carrying a frame-shift mutation, a single base (A) deletion at the 3rd codon of amino acid residue 207. The distribution of *TIM1* haplotypes did not differ among the HIV-positives, ESNs, and controls, suggesting that the *TIM1* haplotypes were not associated with the susceptibility or resistance to the HIV-1 infection (Table 1).

TIM1 haplotype and disease status of HIV-1 infection viral load, CD4 cell count, and clinical status

We analyzed viral load, CD4 cell count, and clinical status among the antiretroviral drug-free women at the recruitment by stratifying the individuals according to their *TIM1* genotypes. We found that patients homozygous or heterozygous for the D3-A haplotype showed a tendency towards higher $CD4^+$ cell count ($P = 0.06$) than patients with other genotypes. Further analyses revealed that the patients carrying the D3-A haplotype had lower proportion of AIDS-related symptoms ($P = 0.021$) than the other patients, although the difference was not statistically significant after the correction of P values for multiple testing (Table 2).

We also found that the D3-C haplotype behaved opposite way to the D3-A haplotype, although there were only two nucleotide differences between the D3-A and D3-C haplotypes (Table 1). CD4 cell count was lower in the patients homozygous or heterozygous for the D3-C haplotype than in those with the other genotypes, although the difference did not reach statistical significance ($P = 0.07$). Further analysis on the proportion of AIDS-related symptoms showed marginally significant difference ($P = 0.05$). The other *TIM1* haplotypes did not show any apparent association with the HIV-1 disease status.

TIM1 haplotype and survival status

Because the cross-sectional study demonstrated a possible association of *TIM1* D3-A haplotype with relatively benign disease status of HIV infection, we intended to

Table 1. TIM1 haplotypes found in the Thai population.

	Polymorphic site								Haplotype frequency		
TIM1 haplotype	T>C (Thr158Met)	3 bp deletion (Thr160del)	18 bp deletion (6AA 161-166 del)	C>T (Pro180Leu)	3 bp deletion (Thr201del)	1 bp deletion (frameshift fs207)	A>G (Thr208Ala)	G>T (Thr208Thr)	HIV-infected ($2n = 492$)	ESN#1 ($2n =$ 148)	Control#2 ($2n =$ 238)
W-A	T	w	w	C	w	w	G	G	0.018	0	0.008
W-C	T	w	w	C	w	w	A	G	0.002	0	0
D1	C	del	w	T	w	w	A	T	0.016	0.020	0.008
D3-A	C	w	del	C	w	w	A	G	0.652	0.676	0.697
D3-C	T	w	del	C	w	w	G	G	0.112	0.149	0.092
D3-C*	T	w	del	C	w	del	G	G	0.002	0	0
D4	T	w	w	C	del	w	A	G	0.205	0.155	0.193

#1; exposed seronegative individuals. #2; healthy blood donors.

Table 2. Clinical parameters of HIV-1 infected individuals stratified by the presence of each TIM1 haplotype.

	D1		D3-A		D3-C		D4		W-A	
	Presence $n=8$	Absence $n=238$	Presence $n=204$	Absence $n=42$	Presence $n=52$	Absence $n=194$	Presence $n=85$	Absence $n=161$	Presence $n=7$	Absence $n=239$
Median viral load (log_{10})	5.45	5.06	5.05	5.11	5.20	5.02	5.08	5.07	5.19	5.07
[IQR]	[4.95–5.90]	[4.28–5.55]	[4.33–5.57]	[4.28–5.51]	[4.54–5.55]	4.25–5.57]	[4.28–5.51]	[4.39–5.57]	[4.25–5.44]	[4.33–5.57]
P	0.0814		0.5975		0.2736		0.6323		0.9635	
Median CD4 cell count	169	266	278	169	174	275	270	262	258	262
cell/μl [IQR]	[48–356]	[71–422]	[90–437]	[50–371]	[52–374]	[94–422]	[76–416]	[66-421]	[25–354]	[71–422]
P	0.3909		0.0615		0.067		0.826		0.304	
HIV-1 related symptoms % (*n*)	62.5 (5)	38.2 (91)	35.8 (73)	54.8 (23)	50.9 (27)	35.8 (69)	40.0 (34)	38.5 (62)	57.1 (4)	38.5 (92)
P	0.155		0.021		0.05		0.819		0.2686	
Death (*n*)	3	62	49	16	18	47	24	41	1	64
PYO	12.58	511.93	443.47	81.03	105.60	418.90	179.94	344.56	17.33	507.17
Mortality rate (%)	23.85	12.11	11.05	19.75	17.05	11.22	13.34	11.90	5.77	12.62
(95%CI)	(−0.26,47.96)	(9.28,14.94)	(8.13,13.97)	(11.08,28.42)	(9.86,24.24)	(8.19,14.25)	(8.36,18.32)	(8.48,15.32)	(−5.31,16.85)	(9.73,15.51)

IQR; Interqualtile range, PYO; person years of observation. W-C and D3-C* were not shown because only one heterozygote was observed.

investigate the association of *TIM1* D3-A haplotype with the disease progression to AIDS. Among 246 HIV-positive individuals, we obtained follow-up information from 238 individuals (96.7%) with the median (inter-quaternary range) of follow-up day at 964 (495-1072) days. The details of follow-up information were reported in our previous study [16]. During the follow-up period, 65 cases died. When we used death as a marker for the disease progression to AIDS, we found that mortality rate of patients possessing the D3-A haplotype was slightly lower than the other patients (Table 2). Kaplan–Meier analysis showed significantly better survival for the D3-A haplotype-carriers than the others ($P=0.044$, log-rank test) (Fig. 1a).

In addition, during the follow-up period, 55 patients had started antiretroviral drug treatment. To adjust the possible effects of antiretroviral treatment on survival, we subtracted the number of days after the patients started the antiretroviral drug from the observation period. As shown in Fig. 1b, we obtained almost identical results to those shown in Fig. 1a. The statistical significance of better survival of patients carrying the D3-A haplotype was found ($P=0.019$), even after the adjustment for the effect of antiretroviral treatment. We also compared the survival prognosis between the homozygous and heterozygous D3-A haplotype carriers for the possible gene dosage effect, but no difference in the survival curves between them was observed (data not shown). These results suggested that the D3-A haplotype could exert a dominant effect on the HIV-1 diseases progression. On the contrary, Kaplan–Meier analysis showed that no other haplotypes significantly affected the survival prognosis in our population samples (data not shown).

The risk of death for patients carrying the D3-A haplotype during the untreated period was significantly lower than the other patients [hazard ratio (HR) = 0.51, Cox model; 95% confidential interval (CI) = 0.29–0.90]. HR conferred by the D3-A haplotype did not significantly change after the adjustment for age (HR = 0.52; 95% CI = 0.29–0.92), plasma viral load (HR = 0.51; 95% CI = 0.29–0.91), or the presence of other risk factors, *RANTES-28G* (HR = 0.56; 95% CI = 0.31–0.99) or *IL4–589T* (HR = 0.47; 95% CI = 0.27–0.84), in which we previously observed apparent protective effects against the disease progression in the same set of samples [16]. On the contrary, adjustment for the baseline CD4 cell count diminished the significant protective effect of D3-A haplotype (HR = 0.72; 95% CI = 0.40–1.28), suggesting that the protective effect conferred by the D3-A haplotype may be due to its effect on the CD4 cell count.

TIM1 D3-A haplotype and the expression of *TIM1*

We investigated the association between the *TIM1* haplotypes and the expression levels of *TIM1* in B

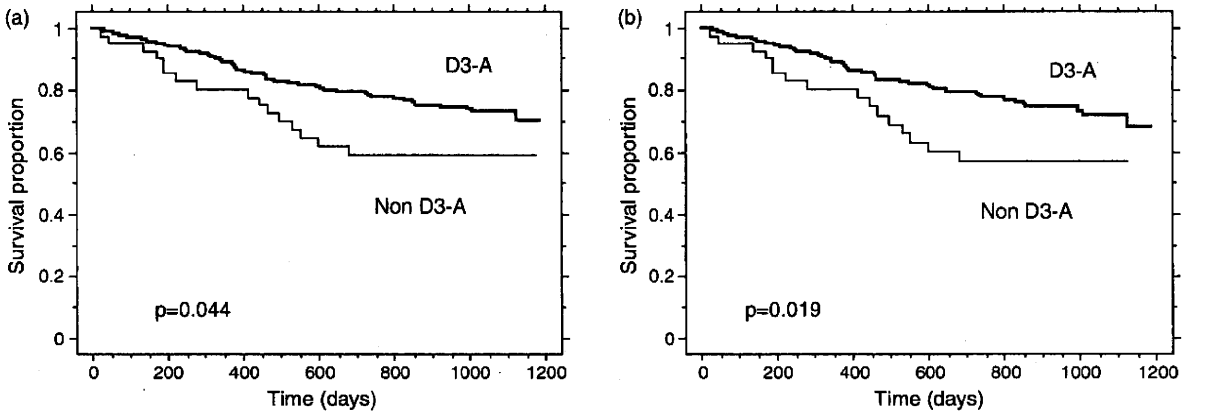

Fig. 1. Kaplan–Meier analysis of the effect of *TIM1* haplotype on the disease progression of HIV-1/AIDS. Kaplan–Meier analyses on the survival in the antiretroviral drug-free HIV-1 infected Thai females during the total follow-up period (a) or untreated period (b). In (a) and (b), patients were stratified by the presence and absence, respectively, of the D3-A haplotype.

lymphoblastoid cell lines. The amounts of *TIM1* mRNA were normalized by *GAPDH* mRNA among 22 cell lines. As shown in Fig. 2a, the cell lines homozygous or heterozygous for the D3-A haplotype expressed significantly lower levels of *TIM1* than those with other genotypes [D3-A carrier ($n=14$) vs. noncarrier ($n=8$); 5.49 ± 2.10 AU vs. 7.56 ± 1.85 AU, $P=0.042$, two-tailed Mann–Whitney test).

We also analyzed the associations of two tightly linked promoter sequence variations, rs7702919 and rs41297577, with the expression levels of *TIM1*. Although these two promoter SNPs were reported to be significantly associated with higher expression levels of *TIM1* [13], we could not replicate the associations; there was virtually no difference in the *TIM1* expression depending on the SNP genotypes or SNP haplotypes (Fig. 2b and c).

Discussion

We demonstrated that *TIM1* D3-A haplotype was associated with slower progression to HIV-related disease in a Thai cohort. Although the statistical significance for the association of D3-A haplotype with HIV-related symptoms in the cross sectional study was lost after the

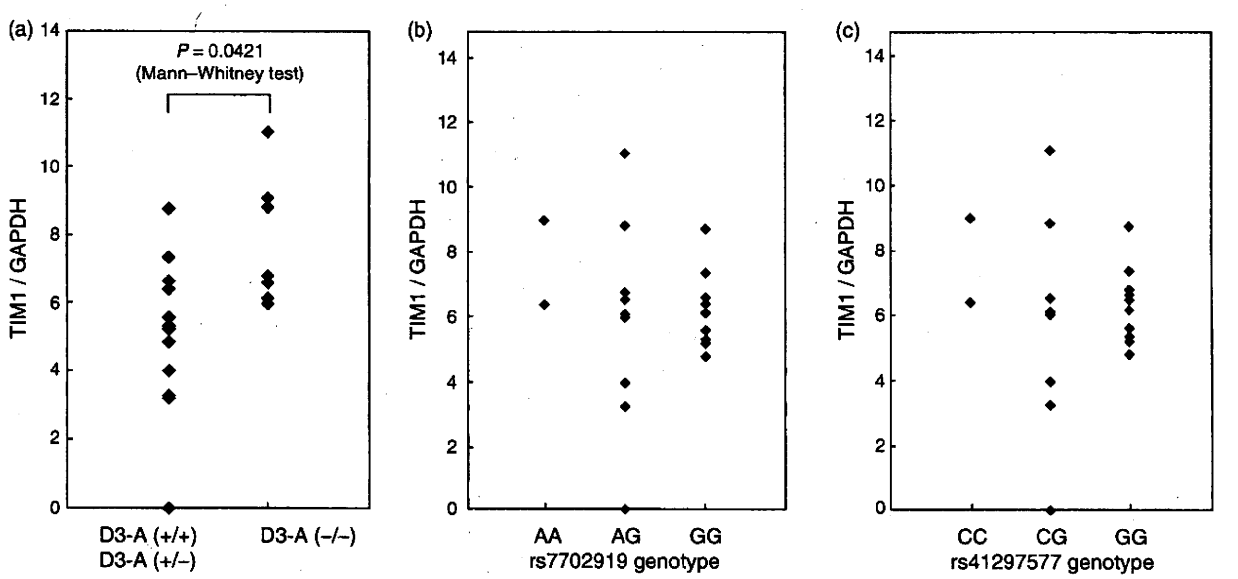

Fig. 2. Correlation between the *TIM1* polymorphisms and the expression levels of *TIM1* in B lymphoblastoid cell lines. Expression levels of *TIM1* were represented by cycle threshold values calculated from quantitative real-time PCR evaluation for *TIM1* transcripts normalized by the *GAPDH* transcripts. The ratio of *TIM1/GAPDH* was used to compare the expression levels in different B cell lines stratified by the presence or absence of D3-A haplotype (a), rs7702919 genotype (b), and rs41297577 genotype (c).

adjustment for multiple testing, Kaplan–Meier analysis showed that the patients carrying the D3-A haplotype followed a better survival prognosis during the untreated clinical course than the others. We also found that the *TIM1* expression level was lower in the cells with the D3-A haplotype than those without D3-A haplotype.

It has been reported that *TIM1* was expressed in the Th2 type $CD4^+$ cells and played crucial roles in the regulation of Th1/Th2 balance by promoting Th2 cells and augmenting Th2 cytokine production [1,2]. A six-amino-acid insertion/deletion polymorphism, which is tightly linked to the D3-A haplotype (Table 1), has been reported to be associated with the susceptibility to atopic disease in HAV-seropositive individuals [8–12]. It is suggested that the effect on Th1/Th2-subset differentiation appears to be a plausible mechanism how the *TIM1* polymorphism determines the susceptibility to atopic disease, because this polymorphism did not affect the infectious rates of HAV. It follows from these lines of evidence that the *TIM1* D3-A haplotype might be associated with low levels of Th2 promotion due to low expression of *TIM1*. Low levels of Th2 promotion would result in enhanced Th1 type responses. It is possible that the enhanced Th1 type immune responses in the HIV-1 infected individuals promote proliferation of CCR5-expressing $CD4^+$ cells, which can enhance the replication of HIV-1 in the infected cells and lead to the rapid progression to AIDS.

On the contrary, however, it is also possible that Th1 type immune responses may promote the proliferation of cytotoxic T cells that can suppress the HIV-1 replication in the infected individuals and lead to the slow progression to AIDS as observed in the study presented here. In the present study, we observed that individuals carrying the D3-A haplotype possessed relatively increased number of $CD4^+$ cells (Table 2) and $CD8^+$ cell (data not shown) at the baseline. It has been reported that in-vitro stimulation of $CD4^+$ T cells with a *TIM1*-specific monoclonal antibody enhanced the T-cell proliferation, suggesting that *TIM1* haplotypes and the expression levels of *TIM1* might be linked to $CD4^+$ and/or $CD8^+$ T-cell counts. It is thus necessary to analyze the number of $CD4^+$ T cells and the proportion of Th1/Th2 $CD4^+$ T cells in individuals with different *TIM1* haplotypes to clarify the effect of D3-A haplotype on the regulation of Th1/Th2 balance in the initial course of HIV-1 infection.

Nuchnoi *et al.* [13] reported an association of *TIM1* promoter haplotypes with the susceptibility to cerebral malaria. They also reported that the promoter haplotype associated with the resistance to cerebral malaria showed a higher expression of *TIM1*. We, however, could not replicate the associations of promoter SNPs with the *TIM1* expression in this study. We also studied the structure of linkage disequilibrium in *TIM1* by using three ethnic population samples from African–American, Caucasian, and Japanese. Sequence variations in exon 4 of *TIM1* were not in significant linkage disequilibrium with the promoter SNPs (data not shown). These observations suggested that the association between the D3-A haplotype and *TIM1* expression was not depending on the promoter SNPs.

Among 439 Thais analyzed in the present study, we identified a novel frame-shift mutation, a single base (A) deletion at the 3rd-codon of amino acid residue 207. This deletion causes a premature termination of TIM1 protein, resulting in a production of aberrantly truncated protein of 220 amino acids long. Therefore, individuals with this rare allele would produce nonfunctional TIM1, because the truncated protein should lack the transmembrane region and cytoplasmic tail. The effect of this frameshift mutation on the HIV-1 infection and/or disease progression to AIDS may be interesting, but we could not obtain definite findings, because there was only one case with this mutation. Further epidemiological studies using larger population samples are required to clarify the impact of the frameshift mutation on the susceptibility to HIV-1/AIDS.

There are several limitations in our study. First, accurate time of HIV infection and dates of seroconversion were not available in our HIV-infected individuals. To study the exact effects of *TIM1* haplotypes on the disease progression and survival time, information on the HIV infection and seroconversion will help further inspections. Second, this is the first report of the association. It is hence to investigate another cohort to replicate the finding. Third, our cohort was composed of HIV-infected women and there might be sex difference. Then, it is worth testing whether the effect of *TIM1* haplotypes could be found in male cohorts. Finally, this study was performed in a Thai population. Because the contribution of a genetic factor could be different depending on the races or ethnic groups, study in other ethnic groups is needed to further confirm the association of *TIM1* haplotypes with the disease status and/or disease progression of HIV/AIDS.

In conclusion, we revealed that a common *TIM1* haplotype D3-A was associated with the relatively slow disease progression in HIV-infected Thai women. We also demonstrated that this haplotype was linked to the decreased expression of *TIM1*. These observations suggested that the *TIM1* haplotype might have impacts on the susceptibility to HIV-1/AIDS via altered Th1/Th2-subset differentiation.

Acknowledgements

We are grateful to all the patients participated in the Lampang cohort and blood donors for their allowing us using their blood in this study and medical staff in Lampang Hospital for their cooperation. We thank Dr Taeko Naruse (Tokyo Medical and Dental University) for

kindly providing us with human B lymphoblastoid cell lines. This work was supported in part by research grants from the Department of Medical Sciences, Ministry of Public Health, Thailand, the Japanese Foundation for AIDS prevention, the Ministry of Health, Labor and Welfare, Japan, the Japan Health Science Foundation, the program of Founding Research Centers for Emerging and Reemerging Infection Disease, Grant-in-Aids for Scientific research from the Ministry of Education, Culture, Sports, Science, and Technology (MEXT), Japan, and a grant from Heiwa Nakajima Foundation, Japan.

References

1. McIntire JJ, Umetsu SE, Akbari O, Potter M, Kuchroo VK, Barsh GS, *et al.* **Identification of *Tapr* (an airway hyperreactivity regulatory locus) and the linked *Tim* gene family.** *Nature Immunol* 2001; **2**:1109–1116.
2. Myers JH, Sabatos CA, Chakravarti S, Kuchroo VK. **The TIM gene family regulates autoimmune and allergic diseases.** *Trends Mol Med* 2005; **11**:362–369.
3. Feigelstock D, Thompson P, Mattoo P, Zhang Y, Kaplan GG. **The human homolog of HAVcr-1 codes for a hepatitis A virus cellular receptor.** *J Virol* 1998; **72**:6621–6628.
4. Ichimura T, Bonventre JV, Bailly V, Wei H, Hession CA, Cate RL, Sanicola M. **Kidney injury molecule 1 (KIM1), a putative epithelial cell adhesion molecule containing a novel immunoglobulin domain is up-regulated in renal cells after injury.** *J Biol Chem* 1998; **273**:4135–4142.
5. Curtiss M, Colgan J. **The role of the T-cell costimulatory molecule Tim-1 in the immune response.** *Immunol Res* 2007; **39**:52–61.
6. Khademi M, Illes Z, Gielen AW, Marta M, Takazawa N, Baecher-Allan C, *et al.* **T cell Ig- and mucin-domain-containing molecule-3 (TIM-3) and TIM-1 molecules are differentially expressed on human Th1 and Th2 cells and in cerebrospinal fluid-derived mononuclear cells in multiple sclerosis.** *J Immunol* 2004; **172**:7169–7176.
7. Nakajima T, Wooding S, Satta Y, Jinnai N, Goto S, Hayasaka I, *et al.* **Evidence for natural selection in the HAVCR1 gene: high degree of amino-acid variability in the mucin domain of human HAVCR1 protein.** *Genes Immun* 2005; **5**:398–406.
8. Gao PS, Mathias RA, Plunkett B, Togias A, Barnes KC, Beaty TH, Huang SK. **Genetic variants of the T-cell immunoglobulin mucin 1 but not the T-cell immunoglobulin mucin 3 gene are associated with asthma in an African American population.** *J Allergy Clin Immunol* 2005; **115**:982–988.
9. McIntire JJ, Umetsu SE, Macaubas C, Hoyte EG, Cinnioglu C, Cavalli-Sforza LL, *et al.* **Immunology: hepatitis A virus link to atopic disease.** *Nature* 2003; **425**:576–1576.
10. Graves PE, Siroux V, Guerra S, Klimecki WT, Martinez FD. **Association of atopy and eczema with polymorphisms in T-cell immunoglobulin domain and mucin domain-IL-2-inducible T-cell kinase gene cluster in chromosome 5q33.** *J Allergy Clin Immunol* 2005; **116**:650–656.
11. Chae SC, Song JH, Heo JC, Lee YC, Kim JW, Chung HT. **Molecular variations in the promoter and coding regions of human Tim-1 gene and their association in Koreans with asthma.** *Hum Immunol* 2003; **64**:1177–1182.
12. Noguchi E, Nakayama J, Kamioka M, Ichikawa K, Shibasaki M, Arinami T. **Insertion/deletion coding polymorphisms in hHAVcr-1 are not associated with atopic asthma in the Japanese population.** *Genes Immun* 2003; **4**:170–173.
13. Nuchnoi P, Ohashi J, Kimura R, Hananantachai H, Naka I, Krudsood S, *et al.* **Significant association between *TIM1* promoter polymorphisms and protection against cerebral malaria in Thailand.** *Ann Hum Genet* 2008; **72**:327–336.
14. Romagnani S, Del Prete G, Manetti R, Ravina A, Annunziato F, De Carli M, *et al.* **Role of TH1/TH2 cytokines in HIV infection.** *Immunol Rev* 1994; **140**:73–92.
15. Klein SA, Dobmeyer JM, Dobmeyer TS, Pape M, Ottmann OG, Helm EB, *et al.* **Demonstration of the Th1 to Th2 cytokine shift during the course of HIV-1 infection using cytoplasmic cytokine detection on single cell level by flow cytometry.** *AIDS* 1997; **11**:1111–1118.
16. Wichukchinda N, Nakayama EE, Rojanawiwat A, Pathipvanich P, Auwanit W, Vongsheree S, *et al.* **Protective effects of IL4-589T and RANTES-28G on HIV-1 disease progression in infected Thai females.** *AIDS* 2006; **20**:189–196.
17. Wichukchinda N, Nakayama EE, Rojanawiwat A, Pathipvanich P, Auwanit W, Vongsheree S, *et al.* **Effects of CCR2 and CCR5 polymorphisms on HIV-1 infection in Thai females.** *J Acquir Immune Defic Syndr* 2008; **47**:293–297.

Uttayamakul et al. AIDS Research and Therapy 2010, 7:8
http://www.aidsrestherapy.com/content/7/1/8

AIDS RESEARCH AND THERAPY

RESEARCH Open Access

Effects of *CYP2B6* G516T polymorphisms on plasma efavirenz and nevirapine levels when co-administered with rifampicin in HIV/TB co-infected Thai adults

Sumonmal Uttayamakul[1,2], Sirirat Likanonsakul[2], Weerawat Manosuthi[2], Nuanjun Wichukchinda[3], Thareerat Kalambaheti[1], Emi E Nakayama[4], Tatsuo Shioda[4], Srisin Khusmith[1*]

Abstract

Background: Cytochrome P450 2B6 *(CYP2B6)* metabolizes efavirenz and nevirapine, the major core antiretroviral drugs for HIV in Thailand. Rifampicin, a critical component of tuberculosis (TB) therapy is a potent inducer of CYP enzyme activity. Polymorphisms of *CYP2B6* and *CYP3A4* are associated with altered activity of hepatic enzyme in the liver and pharmacokinetics resulting in treatment efficacy. This study aimed to investigate whether *CYP2B6* or *CYP3A4* polymorphisms had effects on plasma efavirenz and nevirapine concentrations when co-administered with rifampicin in HIV/TB co-infected Thai adults.

Results: We studied 124 rifampicin recipients with concurrent HIV-1/TB coinfection, receiving efavirenz (600 mg/day) (n = 65) or nevirapine (400 mg/day) (n = 59) based antiretroviral therapy (ART). The frequencies of GG, GT and TT genotypes of *CYP2B6*-G516T were 38.46%, 47.69% and 13.85% in efavirenz group and 44.07%, 52.54% and 3.39% in nevirapine group, respectively. The mean 12-hour post-dose plasma efavirenz concentration in patients with TT genotype at weeks 6 and 12 of ART and 1 month after rifampicin discontinuation (10.97 ± 2.32, 13.62 ± 4.21 and 8.48 ± 1.30 mg/L, respectively) were significantly higher than those with GT (3.43 ± 0.29, 3.35 ± 0.27 and 3.21 ± 0.22 mg/L, respectively) ($p < 0.0001$) or GG genotypes (2.88 ± 0.33, 2.45 ± 0.26 and 2.08 ± 0.16 mg/L, respectively) ($p < 0.0001$). Likewise, the mean 12-hour post-dose plasma nevirapine concentration in patients carrying TT genotype at weeks 6 and 12 of ART and 1 month after rifampicin discontinuation (14.09 ± 9.49, 7.94 ± 2.76 and 9.44 ± 0.17 mg/L, respectively) tended to be higher than those carrying GT (5.65 ± 0.54, 5.58 ± 0.48 and 7.03 ± 0.64 mg/L, respectively) or GG genotypes (5.42 ± 0.48, 5.34 ± 0.50 and 6.43 ± 0.64 mg/L, respectively) ($p = 0.003$, $p = 0.409$ and $p = 0.448$, respectively). Compared with the effects of *CYP2B6*-516TT genotype, we could observe only small effects of rifampicin on plasma efavirenz and nevirapine levels. After 12 weeks of both drug regimens, there was a trend towards higher percentage of patients with *CYP2B6*-TT genotype who achieved HIV-1 RNA levels <50 copies/mL compared to those with GT or GG genotypes. This is the first report to demonstrate the effects of *CYP2B6* G516T polymorphisms on plasma efavirenz and nevirapine concentrations when co-administered with rifampicin in HIV/TB co-infected Thai adults.

Conclusions: *CYP2B6*-TT genotype had impact on plasma efavirenz and nevirapine concentrations, while rifampicin co-administration had only small effects.

* Correspondence: tmskm@mahidol.ac.th
[1]Department of Microbiology and Immunology, Faculty of Tropical Medicine, Mahidol University, Bangkok, Thailand

Background

Tuberculosis (TB) is the most common opportunistic infections in human immunodeficiency virus (HIV) infected individuals, accounting for more than 30% in Thailand, and up to 50% of them die during treatment [1]. The mortality is reduced in HIV-TB co-infected patients who have started the combination antiretroviral therapy after diagnosis of TB [2]. Concomitant administration of highly active antiretroviral therapy (HAART) and anti-TB medications is often complicated due to the drug-drug interaction and the adverse effect profile. Efavirenz and nevirapine based HAART regimens have mostly recommended to use as components of first-line antiretroviral drug regimens worldwide [3]. As efavirenz and nevirapine are potent non-nucleoside reverse transcriptase inhibitors (NNRTIs), they are the preferable option for initial antiretroviral treatments (ART) in HIV/TB co-infection. Rifampicin is a critical component of TB therapy while it is a potent inducer of cytochrome P450 (CYP) enzyme activity [4]. The available pharmacokinetic data showed that rifampicin reduced the plasma concentration of efavirenz and nevirapine of 13-25% and 40%, respectively [5-7]. Recently, efavirenz was shown *in vitro* to be primarily metabolized by hepatic CYP2B6, with minor contributions from CYP3A4 and CYP2A6 [4,8]. While rifampicin is an inducer of CYP3A4, nevirapine induces more CYP2B6 than CYP3A4 [9]. Nevirapine was also shown to be principally metabolized by CYP3A4 and CYP2B6 [10]. *CYP2B6* and *CYP3A4* genotypes are evidenced to be associated with altered activity of hepatic enzyme in the liver and pharmacokinetics that may influence efficacy of treatment, since rifampicin causes decrease in efavirenz and nevirapine concentrations [11-13].

The *CYP2B6* and *CYP3A4* genes are highly polymorphic [14] and are subject to pronounce interindividual variability in expression and activity. A single nucleotide polymorphism (SNP) at position 516 on the *CYP2B6* gene has been widely reported to play an important role in the metabolism of antiretroviral drugs [15-18]. This *CYP2B6* genetic variant affects the efavirenz and nevirapine pharmacokinetics [16,19,20] and associated with clinical response to nevirapine-containing regimens in children [16]. Significant advances have led to a greater understanding of interactions between genetic and host factors that influence the efficacy and toxicity of efavirenz [19,21]. However, the findings from one population may not be generalised to other populations due to the ethnic differences in drug effect and body weight of the patients. In Thailand, it has been recently reported that *CYP2B6*-G516T polymorphism significantly affected the drug metabolism of efavirenz in HIV-infected Thai children [22], while its impact on nevirapine concentrations was less pronounced after intra-partum single-dose nevirapine in HIV-infected mothers [23]. As efavirenz or nevirapine-based HAART is being used as the main therapy in Thailand, however, limited information was obtained so far among various Thai population regarding the influence of host genetic polymorphism on these drug levels especially nevirapine when co-administered with rifampicin which is essential for optimization of ARV dosage or drug-drug interaction. Therefore, the main objective of the present study is to investigate whether *CYP2B6* and *CYP3A4* polymorphisms could influence the plasma efavirenz and nevirapine levels when co-administered with rifampicin in HIV/TB infected Thai adults. The evaluation of clinical and immunological outcomes was also aimed.

Methods

Patients

One hundred and twenty four rifampicin recipients with concurrent HIV-1/TB coinfection were studied. Sixty-five of them received efavirenz (600 mg/day) based ART while 59 received nevirapine (400 mg/day) based ART. Initially, 142 patients were recruited for the study on a randomized control trial to compare the efficacy of efavirenz and nevirapine among HIV-infected patients receiving rifampicin at Bamrasnaradura Infectious Diseases Institute (BIDI), Nonthaburi since December 2006 [24]. They are ARV naïve with active tuberculosis and received rifampicin containing anti-TB regimens for 4-6 weeks prior to enrolment. The patients received oral lamivudine (150 mg) and stavudine (30 mg for those who weighed ≤ 60 kg and 40 mg for those who weighed >60 kg) every 12 hours. They were randomized to receive either efavirenz 600 mg at bedtime while fasting or nevirapine 200 mg every 12 hours after 2 weeks at a starting dose of 200 mg every 24 hours. The dosage of rifampicin was 450 mg/day for patients who weighed ≤ 50 kg and 600 mg/day for those who weighed >50 kg. The anti-TB drug regimen was isoniazid, rifampicin, ethambutol and pyrazinamide for the first two months, followed by isoniazid and rifampicin for the subsequent 4-7 months. Among 142 patients recruited, 25 patients (9 in the efavirenz group and 16 in the nevirapine group) failed to continue the study because of hepatitis (2 cases in the nevirapine group), skin rash (3 in the efavirenz group and 2 in the nevirapine group), death (2 in the efavirenz group and 6 in the nevirapine group), transfer to the other hospital (1 in the nevirapine group), or lost to follow up (4 in the efavirenz group and 5 in the nevirapine group). In the present study, we analyzed 124 patients who have a complete data set of plasma drug levels at week 6 and 12 of ART and 1 month after rifampicin discontinuation. The study was approved by Institutional Ethics Committees of Bamrasnaradura Infectious Diseases Institute and the Ministry

of Public Health, Thailand and the written informed consents were obtained from all participants.

Blood samples

EDTA bloods were collected from patients for SNP genotyping, CD4 T cell counts and HIV-1 viral load. Lithium heparinized bloods were collected after 12 hours of drug administration (C_{12}) at weeks 6 and 12 of ART and after rifampicin discontinuation for 1 month for analysis of plasma efavirenz and nevirapine concentrations. The plasma were separated by centrifugation at 1800 g for 20 minutes and stored at -20°C.

SNP genotyping of *CYP2B6* and *CYP3A4*

The genomic DNA was extracted by using QIAamp DNA blood Mini kit (QIAGEN, Hilden, Germany) and stored at -20°C for SNP genotyping. Genotyping of allelic variants in *CYP2B6* and *CYP3A4* were carried out by real-time PCR using the allelic-specific fluorogenic 5' nuclease chain reaction assay by ABI PRISM 7500 sequence detection system (Applied Biosystems, Foster City, CA) as described previously [15]. Seven SNPs were genotyped: 4 SNPs of *CYP2B6*-G516T, -C777A, -A415G and -C1459T and 3 SNPs of *CYP3A4*-T566C, -T878C and C1088T. Each 25 μl PCR mixture contained 20 ng of genomic DNA, 900 nM primers, 200 nM TaqMan minor groove binder (MGB) probes and 12.5 μl TaqMan universal PCR master mix. The thermal cycler program was set up at 95°C for 10 minutes, and then repeated 40 cycles with 95°C for 15 seconds and 60°C for 1 minute. The plate was read by the allelic discrimination settings. The SNP assay was set up using SDS, version 1.3.0 as an absolute quantification assay. Post-assay analysis was done by using SDS software.

Determination of plasma efavirenz and nevirapine concentration

Plasma efavirenz and nevirapine concentrations were measured by reverse phase high performance liquid chromatography (HPLC) method at the HIV-Netherlands-Australia-Thailand (HIV-NAT) Research Pharmacokinetic Laboratory, Chulalongkorn Medical Research Center (Bangkok, Thailand). HPLC was performed in accordance with the protocol developed by Department of Clinical Pharmacology, University Medical Center Nijmegan (Nijmegan, the Netherlands) [25].

CD4 T lymphocyte counts and plasma HIV-1 RNA quantitation

The CD4 T lymphocyte counts were done at baseline and every 12 weeks after initiation of antiretroviral treatment by flow cytometry using monoclonal antibodies with three colors reagent (TriTEST, Becton Dickinson BioSciences, USA) and analyzed by FACScan flow cytometer (Becton Dickinson BioSciences, USA.). Plasma HIV-1 RNA was determined by RT-PCR at baseline and every 12 weeks after initiation of ART and quantified using the COBAS Amplicor, version 1.5 (Roche Diagnostics, USA). The lower detection limit for HIV-1 RNA level is 50 copies/mL.

Statistical analysis

The different genotypes in relation to plasma drug levels were analysed by SPSS software version 14.0 (ID 5038562) (SPSS Inc., Chicago, IL, USA). If unpaired one-way analysis of variance (ANOVA) was significant ($p < 0.05$), then post hoc Scheffe's *F* test was applied for multiple comparison. When plasma drug levels of different time points were compared, paired T test was used. The CD4 T cell counts and HIV-1 viral load in patients carrying different genotypes were compared by Kruskal-Wallis test. A difference in proportion of patients who achieved plasma HIV-1 RNA < 50 copies/ml at week 12 of ART was evaluated by Chi square or Fisher's exact test. A *p* value of < 0.05 was considered statistically significant.

Results

Patient characteristics

The baseline characteristics of patients are shown in Table 1. All 124 patients were ethnically Thai and among these, 64.6% and 67.8% were male in efavirenz and nevirapine groups, respectively. The patients had the mean ages of 35.89 ± 8.17 and 38.03 ± 8.60 years and the mean body weights of 53.30 ± 9.79 and 54.39 ± 9.39 kg in efavirenz and nevirapine groups, respectively. Similar levels of laboratory parameters including alkaline phosphatase, aspartate aminotransferase, alanine aminotransferase, total bilirubin and direct bilirubin were seen in both patient groups. However, the levels of alkaline phosphatase among patients carrying TT genotype in efavirenz group were higher than those carrying GG or GT genotypes, but this difference was not statistically significant ($p = 0.085$). The median (interquartile range, IQR) CD4 T lymphocyte counts were similar in both groups. In nevirapine treatment group, the log number of plasma HIV-1 viral load among patients carrying GG, GT and TT genotypes seem to be significantly different ($p = 0.041$).

Frequencies of *CYP2B6* and *CYP3A4* genetic polymorphisms

Seven SNPs: 4 SNPs of *CYP2B6*- G516T, -C777A, -A415G and -C1459T and 3 SNPs of *CYP3A4*-T566C, -T878C and -C1088T were genotyped. For *CYP2B6*-G516T, 38.46% (25/65) of GG genotype (wild-type), 47.69% (31/65) of GT genotype (heterozygous mutant) and 13.85% (9/65) of TT genotype (homozygous

Table 1 Baseline characteristics of 124 HIV/TB co-infected patients with *CYP2B6*-G516T genotypes in efavirenz and nevirapine groups.

Baseline characteristics	Efavirenz group (n = 65) *CYP2B6*-G516T				Nevirapine group (n = 59) *CYP2B6*-G516T			
	GG n = 25	GT n = 31	TT n = 9	p-value	GG n = 26	GT n = 31	TT n = 2	p-value
Sex Male: Female	16: 9	21: 10	5: 4	0.795	17: 9	22: 9	1: 1	0.707
Age years, mean (SD)	36.48 (8.08)	35.68 (8.82)	35 (6.63)	0.882	36.48 (8.08)	35.68 (8.82)	35 (6.63)	0.467
Body weight kg, mean (SD)	52.9 (1.87)	53.94 (1.89)	52.22 (3.04)	0.872	54.62 (2.06)	54.7 (1.52)	46.5 (6.5)	0.489
Alkaline phosphatase, U/L, mean (SD)	149.2 (18.38)	137.1 (16.91)	233.9 (68.45)	0.085	150.25 (28.9)	113.97 (11.1)	125 (4)	0.458
Aspartate aminotransferase U/L, mean (SD)	32.8 (2.35)	40.48 (3.32)	43.22 (10.21)	0.202	48.54 (7.31)	35.58 (2.99)	26 (1)	0.167
Alanine aminotransferase, U/L, mean (SD)	27.0 (3.05)	28.55 (2.89)	31.22 (8.89)	0.821	29.81 (3.95)	27.94 (3.57)	23.5 (5.5)	0.877
Total bilirubin, mg/dL, mean (SD)	4.9 (4.34)	0.56 (0.55)	0.43 (0.07)	0.452	2.97 (2.4)	1.13 (0.57)	0.6 (0.1)	0.703
Direct bilirubin, mg/dL, mean (SD)	0.45 (0.14)	0.37 (0.12)	0.21 (0.05)	0.631	0.28 (0.047)	0.52 (0.199)	0.30 (0.1)	0.568
CD4 count, cells/μl, median (IQR)	41 (18-102)	54 (24-120)	67 (12.5-168)	0.818	35.5 (23.5-97)	45 (25-113)	30.5 (23)	0.595
Log Plasma HIV-1 viral load median (IQR)	5.90 (5.57-6.0)	5.93 (5.39-6.0)	5.64 (5.50-6.0)	0.729	5.86 (5.46-6.0)	5.60 (5.41-5.81)	5.80 (Q1 = 5.59)	**0.041***

* Statistically significant by Kruskal-Wallis test. SD: standard deviation. IQR: interquartile range.

mutant) were found among patients in efavirenz group, while in nevirapine group, there were 44.07% (26/59) of *CYP2B6*-516GG genotype, 52.54% (31/59) of GT genotype and 3.39% (2/59) of TT genotype. The genotype frequencies of *CYP2B6*-C777A and -A415G in efavirenz and nevirapine groups were 100% of homozygous mutant AA and 100% of homozygous wild-type AA, respectively. For *CYP2B6*-C1459T, there were 98.5% (64/65) of CC homozygous wild-type and 1.5% (1/65) of CT heterozygous mutant in efavirenz group, and 91.5% (54/59) of CC homozygous wild-type, 6.8% (4/59) of CT heterozygous mutant and 1.7% (1/59) homozygous mutant in nevirapine group. Likewise, the genotype frequencies in *CYP3A4*-T566C and -C1088T were 100% of homozygous wild-type TT and homozygous mutant TT, respectively, in both efavirenz and nevirapine groups. For *CYP3A4*-T878C, there were 95.4% (62/65) of homozygous TT and 4.6% (3/65) of heterozygous TC, and 98.3% (58/59) of homozygous TT and 1.69% (1/59) of heterozygous TC in efavirenz and nevirapine groups, respectively.

CYP2B6-G516T and *CYP3A4-T878C* genetic polymorphisms and plasma efavirenz and nevirapine concentrations

Among 4 SNPs of *CYP2B6*-G516T, -C777A, -A415G and -C1459T being evaluated, the frequencies of wild-type, heterozygous mutant and homozygous mutant were well distributed only in *CYP2B6*-G516T polymorphism, therefore, the analysis of this gene polymorphism was further done in relation to plasma efavirenz and nevirapine levels. The mean plasma efavirenz concentration in patients with homozygous TT genotype at weeks 6 and 12 of ART and 1 month after rifampicin discontinuation (10.97 ± 2.32, 13.62 ± 4.21 mg/L and 8.48 ± 1.30 mg/L, respectively) were significantly higher than those with GT genotype (3.43 ± 0.29, 3.35 ± 0.27 mg/L and 3.21 ± 0.22 mg/L, respectively) or GG genotype (2.88 ± 0.33, 2.45 ± 0.26 and 2.08 ± 0.16 mg/L, respectively) ($p < 0.0001$) (Figure 1a, b, c). Similar results were found in nevirapine group (Figure 1d, e, f) in that the mean plasma drug concentration of patients with TT genotype at weeks 6 and 12 of ART and 1 month after rifampicin discontinuation (14.09 ± 9.49, 7.94 ± 2.76 and 9.44 ± 0.17 mg/L, respectively) tended to be higher than those with GT genotype (5.65 ± 0.54, 5.58 ± 0.48 and 7.03 ± 0.64 mg/L, respectively) or GG genotype (5.42 ± 0.48, 5.34 ± 0.50 and 6.43 ± 0.64 mg/L, respectively) ($p = 0.003$, $p = 0.409$ and $p = 0.448$, respectively).

One month after rifampicin discontinuation, there was a clear trend towards lower plasma efavirenz levels than those during concomitant rifampicin at week 6 and 12 of ART regardless of *CYP2B6* G516T genotypes. In fact, when we evaluated effects of rifampicin on plasma efavirenz levels without stratifying *CYP2B6* G516T polymorphisms, the plasma efavirenz levels after rifampicin

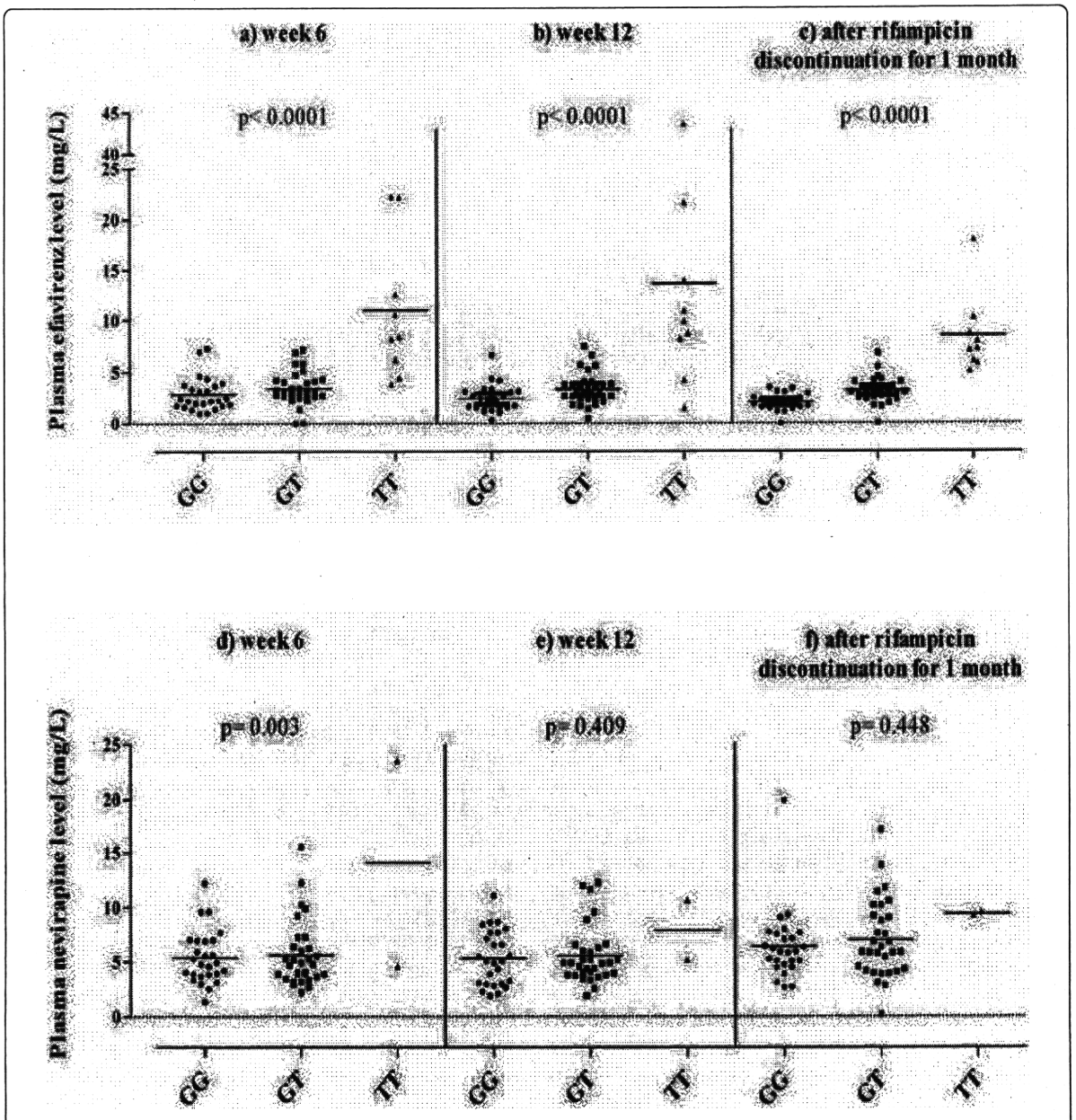

Figure 1 Mean plasma efavirenz and nevirapine concentrations in HIV/TB adults with different genotypes of *CYP2B6*-G516T polymorphism. The scatter diagram of plasma efavirenz (Fig.1a, b, c) and nevirapine distribution (Fig. 1d, e, f) at weeks 6 and 12 of ART and 1 month after rifampicin discontinuation. The numbers of GG, GT and TT genotype patients were 25, 31 and 9 in efavirenz group and 26, 31, 2 in nevirapine group.

discontinuation (3.5 ± 2.67 mg/L) were significantly lower than those at week 6 (4.26 ± 3.96 mg/L) (p = 0.043) and tended to be lower than those at week 12 (4.42 ± 5.97 mg/L) (p = 0.133). In contrast, plasma nevirapine levels at 1 month after rifampicin discontinuation (6.84 ± 3.4 mg/L) were significantly higher than those at week 6 (5.83 ± 3.6 mg/L, p = 0.034) and those at week 12 (5.56 ± 2.63 mg/L, p < 0.001). The reason for these discrepant results on effects of rifampicin on plasma efavirenz and nevirapine levels is not clear at present. Further studies including evaluation of plasma drug levels at time points other than 12-hour post-dose would be thus necessary. Nevertheless, we at least can conclude that the magnitude of effects on plasma